Published in final edited form as:
Nano Today. 2014 April 1; 9(2): 223–243. doi:10.1016/j.nantod.2014.04.008.

Challenges associated with Penetration of Nanoparticles across Cell and Tissue Barriers: A Review of Current Status and Future Prospects

Sutapa Barua and **Samir Mitragotri**[1]
Center for Bioengineering, Department of Chemical Engineering University of California, Santa Barbara, CA 93106

Abstract

Nanoparticles (NPs) have emerged as an effective modality for the treatment of various diseases including cancer, cardiovascular and inflammatory diseases. Various forms of NPs including liposomes, polymer particles, micelles, dendrimers, quantum dots, gold NPs and carbon nanotubes have been synthesized and tested for therapeutic applications. One of the greatest challenges that limit the success of NPs is their ability to reach the therapeutic site at necessary doses while minimizing accumulation at undesired sites. The biodistribution of NPs is determined by body's biological barriers that manifest in several distinct ways. For intravascular delivery of NPs, the barrier manifests in the form of: (i) immune clearance in the liver and spleen, (ii) permeation across the endothelium into target tissues, (iii) penetration through the tissue interstitium, (iv) endocytosis in target cells, (v) diffusion through cytoplasm and (vi) eventually entry into the nucleus, if required. Certain applications of NPs also rely on delivery through alternate routes including skin and mucosal membranes of the nose, lungs, intestine and vagina. In these cases, the diffusive resistance of these tissues poses a significant barrier to delivery. This review focuses on the current understanding of penetration of NPs through biological barriers. Emphasis is placed on transport barriers and not immunological barriers. The review also discusses design strategies for overcoming the barrier properties.

INTRODUCTION

Nanoparticle (NP)-based targeted drug therapies aim to shuttle drugs to the target (diseased) site so as to deliver effective concentrations of therapeutic drugs. The journey of NPs to the desired site, however, is limited by a number of physiological barriers (Fig. 1). These biological barriers are essential components of body's defense system and are designed to limit the penetration of foreign materials. The first barrier to intravenously administered NPs is the reticuloendothelial system comprising the liver and spleen which rapidly remove

[1]Send correspondence to: Professor Samir Mitragotri, Department of Chemical Engineering, University of California, Santa Barbara, CA 93106, Ph: 805-893-7532, Fax: 805-893-4731, samir@engineering.ucsb.edu.

particles from the circulation [1]. Penetration of NPs across the endothelium of the blood vessels into target tissues is another hurdle. Under normal healthy conditions, NPs cannot cross the endothelium of blood capillaries. However, in certain pathological conditions, e.g. inflammation or cancer, endothelial cells lose the cellular integrity due to the activation of proinflammatory cytokines and the gap between the endothelial cells is increased [2]. As a result, NPs can extravasate from the vascular system to the diseased site through the abnormal endothelial gaps.

After escaping from the blood capillaries, NPs face the third level of barrier during their transport through the dense interstitial space and extracellular matrix (ECM) to reach the target cells. The interstitial space is composed of collagen and elastic fiber network of proteins and glycosaminoglycans that form the ECM [3–5]. Interstitial fluid fills the interdispersed spaces within the ECM forming a hydrophilic gel. While the interstitial space and ECM provide the structural integrity to the tissue, in certain diseases, e.g. liver fibrosis and tumor, the collagen content is higher than that of the normal tissue [6]. In this condition, excessive rigidity of the ECM poses a barrier to NPs to transport from the capillaries to the target cells.

The next set of barriers for NPs is the plasma membrane and intracellular localization in the target cells. NPs cannot simply enter the cells *via* diffusion. Instead, they are internalized by endocytic processes including pinocytosis, phagocytosis or endocytosis [7]. The internalization mechanisms depend on NP size, surface properties and types of cells involved. Following internalization, NPs are transported in vesicles from early endosome to late endosomes and eventually to lysosomes. If NPs are able to escape the endosome or lysosome, they diffuse in the cytoplasm and could theoretically enter the nucleus. The nuclear membrane pores do not allow entry of NPs larger than 9 nm [8]. Additional barriers to NP transport also exist if delivery is intended across the skin and mucosal membranes. Both membranes possess outstanding barrier properties and inhibit the transport of foreign materials including NPs.

Despite these cellular- and tissue-level hurdles, a number of NP-based approaches have been developed and hold great promise to transform medicine [9–14]. In the following sections, we describe various biological barriers at the endothelium (section 1), interstitium (section 2), plasma membrane (section 3), skin (section 4) and other mucosal surfaces (section 5). Rational design strategies of NPs to overcome these barriers are discussed for the treatment of various diseases including cancer, arthrosclerosis and dermatological disease. Of the various hurdles, the immunological barriers have been previously discussed in the literature [15, 16]. In particular, the mechanisms of interactions of NPs with macrophages of the RES organs and mechanisms to overcome those hurdles have been reviewed elsewhere [1, 16] and are not discussed here. Instead, this review focuses on *physical* barriers that limit the transport of NPs.

PENETRATION OF NPs ACROSS ENDOTHELIUM

Barrier properties of healthy endothelium

The endothelium comprises a monolayer of endothelial cells that line blood and lymphatic vessels [17]. The endothelium can be continuous, fenestrated or discontinuous [18]. Continuous endothelium is found in most arteries, veins and capillaries of the brain, skin, lungs, heart and muscle. Healthy endothelial cells are anchored to a continuous basal membrane and are connected by tight junctions [17]. The continuous endothelium in normal capillaries ensures seamless diffusion of small molecules such as oxygen and nutrients. However, it limits the transport of NPs into the normal tissue. Fenestrated endothelium is also associated with a continuous basal membrane but contains 50–60 nm wide transcellular channels. The gastrointestinal tract, endocrine and exocrine glands, kidney glomeruli and a sub-group of renal tubules often display fenestrated endothelium. The discontinuous endothelium is associated with a poorly structured basal membrane with 100–200 nm fenestrations without a diaphragm. This occurs in sinusoidal vascular beds predominantly in the liver but also in the spleen and bone marrow [17, 18].

The tightest endothelium in the body is seen in the central nervous system (CNS) in the form of blood-brain barrier (BBB). The BBB is a unique membranous barrier that tightly controls the transport of NPs between the blood and the brain to control the internal environment of the brain [19]. The blood capillaries in the CNS possess different structures than those in other tissues. The endothelial cells of the cerebral capillaries have a particularly impermeable membrane and are separated by ~0.3 μm thick endothelial cytosol [20]. The hydrophilic channel between two adjacent cells is ~0.8 nm. The cells are also characterized by the presence of increased number of mitochondria, lack of fenestrations, minimal content of pinocytosis and the presence of tight junctions. The tightly fused junctions of the cerebral endothelium essentially form a continuous lipid layer that allows passage of only small, electrically neutral, lipid-soluble molecules but is practically inaccessible to NPs. The endothelial cells express a high level of transport proteins to facilitate the essential polar metabolites such as glucose and amino acids. Unlike systemic endothelium, cerebral endothelial cells have a marked deficiency of pinocytosis. The transport of molecules mainly depends on cellular transcytosis. In addition, a large number of drug molecules are removed before entering the CNS by ATP binding cassette C1 (ABCC1) and ABCB1 (also known as p-glycoprotein) drug efflux transporter protein from the cerebrospinal fluid to the blood [21, 22].

Perturbed Endothelial Barrier (EPR effect)

The otherwise healthy and non-permissive epithelium has been shown to permit the transport of NPs under certain pathological conditions. Two key pathologies of relevance to drug delivery are discussed below.

Cancer—The blood vessels surrounding the tumor are leaky and exhibit heterogeneous hyperpermeability and defective lymphatic drainage compared to normal tissues [3, 4]. The leakiness in tumor vasculatures leads to penetration and retention of NPs in the tumor bed which is known as enhanced permeation and retention (EPR) effect. The enhanced

permeability allows NPs to escape the circulation owing to the inherent leakiness of the underdeveloped tumor vasculature. The pore size in the leaky tumor vasculatures has been reported to range from 380 to 780 nm [23, 24]. Therefore, NPs that rely on EPR to target tumors should possess size below this cut-off.

EPR-based NPs are being actively used in medicine [25, 26]. For example, albumin bound paclitaxel (PTX) (Abraxane) NPs have been approved by the FDA for the treatment of breast cancer in 2005 [27]. The size of these NPs is 130 nm which is ideal from the perspective of EPR. Other PTX-loaded polymer conjugates under investigations in clinical trials are PTX-poliglumex in phase III clinical trial for non-small cell lung cancer (NSCLC) [28] and cationic liposomal PTX (EndoTAG-1) in phase II trial for hepatocellular (liver) cancer [29]. Liposomes with a diameter less than 400 nm have been shown to extravasate in a human adenocancer xenograft implanted in nude mice [30]. Doxorubicin-loaded liposomes (Doxil) have been found to accumulate in human tumors based on fluorescence microscopy of patient biopsies [31, 32]. For further details on Abraxane, Doxil and polymeric NPs, please see Refs. [9, 27, 33].

Artheroscelerosis—EPR effect is also found in atherosclerosis which is associated with chronic inflammation of arterial blood vessels [34]. Exposure of the endothelium of the blood vessels to free radicals, hypertension, or oxidized low-density lipoprotein (LDL) leads to the formation of atherosclerosis [35, 36]. With the progression of this disease, the inner lining of arterial blood vessels form atherosclerotic plaques by depositing lipids, cholesterol, cellular waste products, calcium and other substances. The high metabolic activity that is necessary for building the plaques demands elevated nutrition and oxygen supply to the underlying cells. As a result, the endothelial cells proliferate rapidly and form atypical blood vessels that are defective and immature as that seen in tumor blood vessels. The leaky vasculature allows NPs to pass into the interstitial tissue, while an undeveloped lymphatic drainage system increases accumulation and local concentration of drugs.

NPs of different sizes and chemistries have been investigated for localized drug delivery to atherosclerotic plaques. Inflammation of atherosclerotic plaque in rabbits has been treated by delivering prednisolone phosphate drugs encapsulated in PEG-liposome NP formulation [37]. The liposomes accumulate in the plaques *via* the EPR effect. Among polymeric NPs, poly(*D*,*L*-lactide-*co*-glycolide) (PLGA) NPs of 100 nm size demonstrated more than three-fold higher uptake compared to 275 nm size NPs in an *ex-vivo* canine carotid artery model [38]. Polymeric micellar NPs have also shown increased drug delivery to vascular endothelium injuries at porcine aortas due to EPR effect [39]. NPs of cationic block-copolymers have been used to induce transfection of vascular smooth muscle cells [40, 41]. In another study, injured arteries were recovered by delivering PTX using multilayered polymer-lipid NPs (Fig. 2) [42]. Nanoparticulate imaging agents have led to enhanced signals for the detection of atherosclerotic plaques by incorporating image contrast agents such as gadolinium (Gd) [43]. High density lipoproteins (HDLs), in the size range of 7–13 nm, have been used to image macrophages within the atherosclerotic plaques by incorporating Gd [44, 45], gold (Au) nanocrystals [46], iron oxide [47] or quantum dots (QDs) [47, 48].

2.3 Strategies to enhance NP penetration across healthy endothelium

Despite the hurdles imposed by the endothelium, several advances have been made to develop NPs with enhanced ability to cross the endothelium. Some of these advances are discussed below.

Receptor-mediated delivery—This is by far the most explored means of enhancing endothelium penetration. Poly(lactic acid) (PLA) and poly(ethylene glycol) (PEG) block copolymer NPs decorated with an aptamer against prostate specific membrane antigen (PSMA) receptor have been tested in phase I clinical study [49]. Patients with advanced or metastatic cancers were treated with docetaxel (DTX) loaded NPs in order to assess the dose-limiting toxicity and determine the maximum tolerated dose (MTD). The preliminary data showed pharmacokinetic profiles similar to those observed in preclinical studies [49]. One patient responded to a reduction in tumor volume at DTX doses lower than the conventional protocols used in clinical trials. Further studies on safety, biodistribution and pharmacokinetic parameters are required in a larger number of patients. Role of specific targeting in observed pharmacological effects should also be tested. In addition to PSMA, which is found on the surface of tumor neovasculature [50], another overexpressed target in many cancers is transferrin (Tf) receptor (TfR) [51]. TfR-targeted polymer NPs showed increased uptake of small interfering RNA (siRNA) by cancer cells [10, 52, 53]. Patients were treated to inhibit the expression of M2 subunit of ribonucleotide reductase (RRM2) cancer gene by delivering siRNA using a linear cyclodextrin polymer vector, PEG-adamantane and transferrin ligand. In the phase I clinical trial, a reduction in both RRM2 messenger RNA (mRNA) and protein levels were found in tumor biopsies of melanoma patients.

Vascular targeting has been accomplished by functionalizing the NPs to target integrins which are overexpressed in the blood vessels surrounding the atherosclerosis plaques. $\alpha_v\beta_3$ integrin-targeted iron oxide NPs have been developed that utilize EPR effect as well as active targeting to deliver an antiangiogenic drug, fumagillin to the atherosclerosis plaques in a rabbit model [54]. These multifunctional NPs were able to image $\alpha_v\beta_3$ integrins, decrease the concentration of $\alpha_v\beta_3$and deliver fumagillin showing decreased aortic angiogenesis in combination with atorvastatin. A variety of NPs have also been developed by making use of Intercellular Adhesion Molecules, for example, ICAM-1, to target a variety of inflamed endothelium [55].

NPs have also been designed to cross the BBB *via* receptor mediated endocytosis [19, 56, 57]. Various receptors including Transferrin receptor (TfR), Insulin receptor (IR) and low density lipoprotein (LDL) receptors have been studied to enhance transport. PEGylated albumin NPs conjugated to Tf have been shown to increase the percentage of injected NPs in the rat brain compared to the PEGylated NPs without Tf [51]. An antiviral drug, azidothymidine (AZT) crosslinked to Tf-albumin NPs was shown to accumulate in the rat brain. Targeting TfR is cumbersome because the TfR is saturated with a relatively high concentration (25 μM) of endogenous Tf. Therefore, alternate targeting antibody such as a peptidomimetic monoclonal antibody, OX26 has been studied by coupling a PEG spacer in chitosan nanospheres. The NPs were translocated in the brain tissue after intravenous

administration [58]. OX26 binds to a distinct extracellular epitope of the TfR other than Tf binding site which limits the effects on natural Tf transport and prevent competitive binding between Tf ligand and Tf-conjugated drugs.

More effective antibodies (8D3 and RI7–217) have been found than OX26 for brain targeting [59].

Like the TfR, IR is overexpressed on the luminal membrane of brain endothelial cells and undergoes receptor mediated endocytosis across the BBB endothelium [60]. A number of antibodies including 83-14 mouse monoclonal antibody (mAb) against the human IR (HIRmab) have shown efficacy in enhancing transport across BBB in humans [61]. Human serum albumin (HSA) NPs conjugated with an anti-insulin receptor monoclonal antibody (29B4) enabled transport of NPs across the BBB in mice after intravenous injection [62]. NPs coated with polysorbate 80 surfactant have also shown higher penetration of drugs including dalargin, doxorubicin, loperamide and methotrexate that normally cannot cross the BBB [63–66].

Control of NP properties: Size and Shape—The penetration of NPs into tumors is influenced by their size, surface charge and shape. Small NPs enhance tissue penetration but those smaller than 10 nm are cleared by renal excretion and phagocytosis. NPs around 100 nm exhibit enhanced circulation half-life compared to smaller or larger particles. An innovative approach to meet the above two criteria is to formulate multistage NPs such as the gelatin NPs of 100 nm encapsulating 10 nm QD NPs in the core. Gelatin NPs accumulate in the tumor vasculature by the EPR effect and eventually release the 10 nm QDs into the tumor interstitial space [67]. Polystyrene NPs of 20 and 40 nm penetrated the tumor and distributed homogeneously while 100 and 200 nm particles showed restricted penetration [68]. PEGylated phospholipids of 10–20 nm size improved the tumor penetration and anti-cancer efficiency of DOX due to better tumor distribution [68].

Shape also affects biological responses to NPs. The shape of the particles can be spherical, discoidal, rod-like or filamentous, among others [69]. Shape-specific NPs can be engineered using various techniques including film stretching [69], jet and flash imprint lithography (J-FIL) [70], particle replication in non-wetting templates (PRINT) [71, 72] and other nanofabrication processes [73, 74] (for detailed methods, see Refs. [69–74]). Rod-shaped NPs, when coated with herceptin, exhibited higher binding to the HER2-overexpressing breast cancer cells than spherical NPs [75, 76]. Shape has also been shown to induce targeting of antibody-coated NPs to endothelium. Specifically, anti-ICAM-1 or anti-transferrin receptor antibody-coated nanorods exhibited higher specific binding to lung and brain endothelium compared to spherical particles of the same volume (Fig. 3) [77]. The interplay between shape and cell-specificity was critical for cellular uptake. Herceptin-coated nanorods exhibited increased internalization than spherical or disk-shaped NPs in BT-474 breast cancer cells (Fig. 4). Cationic cross-linked PEG hydrogel NPs of 150×450nm were internalized faster than 100×300nm NPs by HeLa cells [71]. Rod-shaped mesoporous silica NPs of 450nm length showed better uptake than 250 nm rods or 100 nm spherical particles by A375 human melanoma cells [78]. Elongated particles were also shown to avoid phagocytosis depending on the contact angle to the macrophages [79], and exhibit long

blood circulation [80]. Biodistribution analysis of silica nanorods demonstrated enhanced lung accumulation than that of uncoated silica nanospheres [81]. The adhesion strength of non-spherical particles towards the blood vessel wall is higher than spherical NPs as shown both experimentally and theoretical modeling [73, 82–85]. Disk-shaped particles also offer an advantage in that they exhibit lateral drift towards the blood vessel wall and adhere more avidly to the vascular walls under flow.

Use of Physical Forces—External forces can also improve NP penetration across the endothelium. Ultrasound (US) is a non-invasive method to deliver drugs into deep tissue without surgical intervention. It can be mediated by two mechanisms: thermal and non-thermal. Non-thermal US generates temperatures < 43°C that is used to sensitize the cancer cells to chemotherapy or radiotherapy. For example, pulsed US enhanced penetration of polystyrene particles [86] into tumor spheroids *in vitro*. US has been shown to increase the delivery of liposomes up to 4.5 fold in epithelial-mesenchymal transition (EMT) tumors compared to the delivery without US [87]. US-activated microbubbles have been used for the delivery of PLGA NPs containing 5-fluorouracil (5-FU) [88]. This improved the delivery of NPs by 5–57 fold compared to the individual treatment or various control groups in glioma xenografts in mice. In addition, 5-FU-carrying NPs decreased the tumor volume by 67% after 7 days of the initial treatment. US exposure enhanced the delivery of galactosylated DTX NPs into the hepatocellular cancer xenografts and inhibited the tumor growth by 74.2% [89].

The thermal US utilizes high temperature (>60°C) for the thermal ablation of the tissue which is also known as focused US (FUS). The FUS treatment has been used to deliver magnetic NPs (MNPs) containing epirubicin across the BBB [90]. The combination treatment of FUS and magnetic treatment deposited ~21.7μg epirubicin per gram of brain tissue, while treatment using FUS alone accumulated only ~1.3μg epirubicin per gram of tissue. FUS exposure after DOX-superparamagnetic iron oxide (SPIO)-microbubble injection increased the local deposition at the brain tumor site by 22.4% compared to 12% accumulation without the magnetic targeting [91]. Gold NPs have also been tested in combination with FUS treatment in order to penetrate the BBB in a rat model [92].

Biological means—Another approach to deliver NPs across the endothelium is to camouflage them within innate cells and escape the body's immune system. One potential strategy is to use biomimetic camouflage in the form of NP and cell-based hybrid systems. Such new systems have been prepared by self-assembly of white blood cells (leukolike vectors or LLVs) and nanoporous silicon NPs (NPS) to avoid opsonization and phagocytosis, but facilitate transport across the endothelium of tumor [93]. The *in vivo* study using LLV-NPS showed delayed accumulation in the liver, and enhanced particle concentration at the tumor site. Delivering NPs on the membrane of red blood cells (RBCs) has also been demonstrated an effective method of drug delivery [94, 95]. The natural biconcave shape of the RBC and their deformability under flow has enabled them to be confined within the core of blood vessels and thus improving drug delivery in the vascular system without crossing the endothelial barrier. Model polymeric NPs non-specifically anchored to RBCs undergo dramatic enhancements in their circulation time compared to

free NPs which are cleared within a few minutes [94]. The RBC-adsorbed NPs have demonstrated 5-fold enhanced accumulation in lung endothelium compared to the free NPs [95]. RBC-adsorbed NPs have also exhibited reduced clearance in spleen compared to free NPs. Once the NPs are delivered to the surface of the target endothelium of microvessels, they may penetrate the endothelium through endocytosis and transcytosis on their own. Attachments of anti-ICAM-1 antibody to RBC-anchored NPs further increased lung targeting and retention over 24 h. RBC-mimicking synthetic polymer particles have been prepared using the layer-by-layer technique [96]. The resulting RBC particles are flexible, and have shown oxygen carrying capacity.

RBC mimicking hydrogel particles have also been prepared using PRINT technology to yield flexible particles that match the elasticity of natural RBCs (Fig. 5) [97]. The circulation half-life of synthetic RBCs was enhanced up to ~93.3 h compared to ~2.9 h for the least flexible particles. Neither of these particles is intended to cross endothelium.

Therapies using immune cells *e.g.*, T cells have established the potential to deliver cytokines to solid tumors or activate immune cells to eliminate the tumor. Migration of gold NP-loaded T-cells into tumors has been tested in a transwell chemotaxis assay in contrast to T-cell migration alone [98]. T cells enhanced the efficiency of gold NPs by four-fold compared to the PEGylated gold NPs. Coupling of polymeric NPs to the surface of T cells via maleimide-thiol conjugation has been used to localize NPs on the cell surface without affecting cellular functions such as *in vivo* migration, cellular proliferation and cell fate [99]. NPs loaded with cytokines interleukin (IL)-15 and IL-21 have been conjugated onto the surface of anti-tumor T cells. When the T-cell-coupled NPs are injected systematically, NPs accumulate at tumor sites where the *in vivo* T-cell expansion is induced leading to the regression of tumor growth (Fig. 6). Similar approach has been tested to successfully deliver growth factors from cell surface-linked NPs for the proliferation of hematopoietic stem cells (HSCs) [99]. Cell-mediated therapies show potent strategies for enhancing therapeutic activity of drugs.

TRANSPORT OF NPs IN TISSUES

NPs after extravasating from the blood capillaries have to reach to the diseased cells prior to rendering their therapeutic effects. The following sections discuss the barriers that influence NP movement to the diseased site.

Factors governing NP transport

Tumor interstitium—The interstitial space is a dynamic and complex environment comprising a matrix of extracellular biomacromolecules, the extracellular matrix (ECM). The ECM consists of a collagen network, microfibrilar elastins, glycosaminoglycan (GAG) and proteoglycans that form a cross-linked gel-like structure. The viscous nature of the interstitium limits the fluid flow and diffusion of NPs from the blood towards the cells. Fluid flows from the capillary filtrate into the extravascular space at a lower velocity (0.1–4 μm/s) than the capillary fluid flow [23].

NPs encounter diffusion limitations in the ECM due to their large size. Studies have shown that the transport of 68 kDa bovine serum albumin (BSA) and 150 kDa immunoglobulin (IgG) is significantly hindered in tumor xenograft models [6]. NPs are 10–20 times bigger than BSA or IgG. Therefore, NPs often accumulate at the periphery of the tumor mass without reaching the core. The tumor stroma is associated with an altered ECM and an increased number of fibroblasts that synthesize growth factors, chemokines and adhesion molecules that further hinder the penetration of macromolecules through the tissue. For further reviews detailing the tumor interstitial space, please see Refs [3, 6].

Dense extracellular matrix—Tumor ECM is denser than the normal ECM due to the presence of high collagen, increased level of lysyl oxidase (LOX), and enhanced integrin receptors [100]. The high collagen levels in the tumor ECM is a major barrier in the transport of NPs [6, 101]. LOX crosslinks collagen and thus stiffens the ECM [101]. Inhibition of LOX decreases collagen crosslinking [101]. Integrin receptors such as $\alpha_v\beta_3$ are overexpressed in melanoma, glioblastoma, breast, prostate, pancreas, ovary and cervical cancers [102]. Integrins promote focal adhesions of cells and cytoskeleton remodeling that influence the tumor cell growth [102]. The ECM also has an increased number of fibroblasts that synthesize growth factors, chemokines and adhesion molecules contributing to tumor cell proliferation [23]. This dense ECM becomes a major barrier to the transport of NPs in solid tumors. In addition, many drugs may bind to the matrix further lowering the transport rates [3].

Distances in the interstitium—NPs may move through the interstitial space by diffusion as well as convection. However, for NPs larger than 4 nm, the mass transport occurs mainly by diffusion [4, 103, 104]. Diffusion of NPs determines both local and global distribution that is hindered by the microporous network of fibrillar collagen and elastin in solid tumor [105]. The properties of NPs including size, shape, surface charge, solubility and surface functionality affect their diffusion [3]. While small chemotherapeutic molecules up to a few nanometers can diffuse through the interstitial space fairly rapidly, NPs such as liposomes and viruses of ~100 nm cannot move within the dense matrix. In fact, NPs larger than 60 nm cannot diffuse through the ECM matrix [106, 107]. The time required to cross the tumor interstitium is. For IgG, values of for the diffusion of IgG are 1 h, ~2 days and ~8 months to cross 100μm, 1mm and 1cm distance, respectively [4].

Interstitial Fluid Pressure (IFP)—IFP leads to a pressure gradient exerted by the exchange of oxygen, nutrients and waste products from the capillaries through the interstitial space into the lymph nodes [3, 4, 103]. It creates a slightly negative pressure (-3 to 3 mm Hg) in normal interstitium that is necessary for tissue homeostasis. In tumor cells, rapid cell proliferation and metabolism requires increased levels of oxygen and nutrients. However, the rate of blood vessel formation is not as fast as the tumor growth. As a result, IFP in tumor is significantly increased ranging from 5 up to 100 mm Hg causing hypoxic conditions in the tumor [108]. High tumor IFP causes an increased outflow of proteins and other molecules from the tumor interstitial vessels to the blood stream. IFP also increases the level of several transcription factors, mainly the hypoxia inducible factor-1 (HIF-1), HIF-1α and HIF-1β. HIF-1 upregulates the glucose transporter proteins for the glycolysis of glucose

molecules into pyruvate which is the main nutrient supply for tumor cells in a hypoxic environment [109].

pH—Tumors exhibit a lower extracellular pH (6.0–7.0) than normal tissues and blood (pH 7.4). In the hypoxic tumor microenvironment, tumor cells produce adenosine triphosphate (ATP) mainly by glycolysis metabolism in an anaerobic environment rather than the tricarboxylic acid (TCA) cycle in aerobic environment [110, 111]. During this two-step process, glucose is metabolized to pyruvate following the conversion of pyruvate to lactic acid. In the second step, a large number of H^+ ions are produced and transported out the cells, thus resulting in acidic environment of the tumor interstitial space. While the pH as such does not alter the transport properties of NPs, it may impact their stability and other relevant properties.

Strategies to facilitate NP transport through the interstitial space

Transport of NPs in tumor interstitium can be enhanced by weakening the dense matrix of ECM and decreasing IFP. One approach is the use of enzymes, e.g. collagenase and hyaluronidase, to weaken the matrix structure [112, 113]. Both of these enzymes have shown improved penetration of IgG and dextran into the tumor [6, 114, 115]. Hyalurodinase has been used to improve the uptake of liposomal DOX (Doxil) in tumors [116]. Both intratumoral and intravenous injection of hyalurodinase decreased IFP by 40% in mice xenograft models. Hyalurodinase enhanced DOX distribution two to eight times higher throughout the whole tumor than Doxil alone without altering the intranuclear transport of DOX. Transport of fluorescent polystyrene NPs (20–200 nm) has been tested in human cervical cancer cell (SiHa) spheroids *in vitro* after collagenase treatment. Smaller (20–40 nm) NPs diffused to the middle quiescent region due to increased porosity and cell loosening by collagenase treatment. NP distribution was limited to the periphery of the spheroid without the collagen treatment [117].

Matrix metalloproteinases (MMPs) mainly MMP2 and MMP9 are upregulated in tumor interstitial space [118]. MMP-sensitive peptide sequences have been developed for the attachment of chemotherapeutic drugs or macromolecules for the delivery to tumor cells. Conjugation of DOX to albumin via MMP-2 sensitive linker has been used for the treatment of A375 human melanoma xenograft [119]. DOX showed moderate inhibition in tumor growth in nude mice indicating active cleavage of the linker for an efficient release of DOX into the melanoma tissue. Similarly, conjugation of methotrexate to dextran to an MMP linker inhibited tumor growth by 80% compared to an MMP-insensitive control in HT-1080 and U-87 *in vivo* tumor models [120]. A multifunctional micelle NP was synthesized using self-assembly of an MMP-2 linker, PEG 2000, PTX drug and phosphoethanolamine (PE) cell penetrating agent. The linker was found to be cleaved off *in vitro* in presence of MMP2 and released PTX showing four fold higher LDH release than free PTX *in vitro*. The *in vivo* efficacy in mice xenografts showed accumulation of the NPs in liver and tumor with a negligible accumulation in heart, spleen, lung and kidney. PTX concentration using MMP2 sensitive linker was 2.5 fold higher than the MMP2 non-sensitive linker in the tumor tissue [121].

Reduction of IFP facilitates the efficient uptake of NPs in tumors. This can be done by enhancing the permeability of vasculatures using nitroglycerin, or increasing the systemic blood pressure using angiotensin II [122–124]. Nitroglycerin enhanced the delivery of PEG-Zinc protoporphyrin (PGP) NPs in cancer tissue by dilating the blood vessels in the tumor [125]. A proinflammatory cytokine tumor necrosis factor-α (TNF-α) causes an increased pressure gradient across the vessel wall and thus increases the delivery PEG-liposomes by 5 to 6-fold [126]. Radiation treatment can also increase the vascular permeability of solid tumors and delivery of NPs [127, 128].

pH responsive NPs are ideal carriers for active targeting and intracellular delivery. Polymeric NPs such as poly(L-histidine) (PHS), PHS-PEG and poly(lactic acid)-*b*-poly(ethylene glycol)-*b*-poly(histidine) (PLLA-b-PEG-*b*-polyHis) are promising vehicles because the imidazole group in histidine is generally ionized at acidic pH and serve as cationic vectors for drug delivery [129]. Polymeric micelles consisting of PHS, PEG and poly(L-lactic acid) (PLLA) have shown pH-dependent DOX release [130]. The DOX-loaded micelles inhibited MCF-7 xenografted tumor 3.6–4.5 times smaller than PBS or DOX-treated mice [131]. An NP system consisting of a pH sensitive polymer and cationic cell penetrating peptide has been developed for longer circulation and drug delivery to tumor tissue [132]. A polymer-virus hybrid was prepared using poly(histidine-co-phenylalanine) core and two layers of hydrophilic shell [133]. The inner shell was prepared using PEG surrounded by BSA outer shell. Folic acid was conjugated to the BSA outer shell for specific interaction with folate receptor proteins overexpressed in many cancer cells [134]. This NP swells in acidic pH and de-swells in neutral pH making it an attractive candidate to release chemotherapeutic drug e.g. DOX in the acidic tumor microenvironment. NPs containing a variety of ester and hydrazone groups conjugated to PEG have been developed since these chemical bonds are stable at pH ~7.4 but hydrolyzed at pH ~ 6.0 [135]. A galactose-PEG (Gal-PEG) NP was designed to conjugate an oligonucleotide (ODN) *via* an acid-labile ester bond, β-thiopropionate.

Dual responsive polymers sensitive to both pH and temperature offer better targeting and efficacy to deliver drugs to complex microenvironment [136]. A pH responsive polymer, modified with undecenoic acid (UA) was used to self-assemble with a temperature sensitive polymer, *N*-isopropylacrylamide (NIPAAm) [136]. UA becomes more hydrophobic due to protonation at low pH (~5). Poly(NIPAAm) is hydrophilic at temperatures below its lower critical solution temperature (LCST) at 32°C, while it becomes hydrophobic above its LCST. The LCST was increased to ~37°C by adding a third polymer, *N*,*N*-dimethylacrylamide (DMAAm). The three polymers were self-assembled and formed core-shell micelle structures (poly(NIPAAm-*co*-DMAAm-*co*-UA)) that encapsulate the PTX anti-cancer drug. The poly(NIPAAm-*co*-DMAAm-*co*-UA) micelles greatly enhanced the therapeutic effect in the mouse hepatocyte cell line, BNL CL.2 by slowly releasing PTX at 37°C, without causing much cytotoxicity in NIH3T3 mouse fibroblast control cells [136].

ENDOCYTOSIS AND SUBCELLULAR TRAFFICKING OF NPS

Specific uptake of NPs in target cells is essential for maximizing efficacy and minimizing toxicity. For specific targeting and internalization, NP surface is usually decorated with

surface targeting moieties such as antibodies, proteins, aptamers, peptides, folate and other small molecules [53, 120, 131, 137]. The surface-modified NPs enter the cell mainly via receptor-mediated endocytosis, caveolae-mediated endocytosis, lipid raft mediated endocytosis and macropinocytosis [7]. For details on endocytosis, please see Ref. [7]. However, gaining access to the cell is not sufficient to maximize the drugs' therapeutic outcomes. Drug molecules must be delivered to the right target by avoiding their lysosomal degradation. After endocytosis, drug molecules can be localized at four major intracellular organelles: the cytoplasm, mitochondria, nucleus and lysosome.

Releasing drugs at the cytoplasm

Drug-carrying NPs that enter the cells are trapped in an endosome which may fuse with other endosomes inside the cells proceeding deeper from the plasma membrane. Release of drugs from the endosomes to the cytosol may occur due to osmotic swelling, direct membrane rupture or other mechanisms [138]. pH sensitive liposomes have been used to release encapsulated calcein and fluorescent dextran to the cytoplasm by destabilization of the liposome and endosomal membrane at acidic pH [139]. Cell penetrating peptides such as transactivating transcriptional activator (TAT) have been shown to release BODIPY ceramide molecules in the cytoplasm [140]. Amphiphathic peptides e.g. GALA, polymers containing disulfide groups, polymers with acid labile acetal groups have been used for the delivery of DNA into the cytosol [141–143]. Polymer NPs were disrupted in the reductive environment of endosomes leading to the disruption of endosomal membrane and thereby releasing the drug/ plasmid DNA. Polycationic polymers, such as hydroxyethyl aspartamide conjugated to histidine also exhibit pH dependent endoosmolytic properties [33]. These polymers have been used to deliver DOX to the nucleus by first releasing the drug in the cytosol. However, the proton sponge mechanism is controversial suggesting that the proton sponge effect may be not the dominant mechanism of the NP escape in the cytoplasm [144]. Light-induced photochemical internalization has shown to trigger endosomal disruption using photosensitizing molecules [145].

It has been found recently that NP shape plays an important role in the process of subcellular targeting of NPs. Herceptin-coated CPT nanorods show differentiation in subcellular targeting after being internalized by BT-474 breast cancer cells. Herceptin is found in the cytoplasm after 2 h of incubation, however, almost all the herceptin recycles back to the plasma membrane after 24 h when delivered as herceptin-CPT nanorods (Fig. 7). Free herceptin remains in the cytoplasm even after 24 h of incubation. CPT nanorods travel further down in the cytoplasm and stop close to the nucleus.

Mitochondria-specific NPs

Mitochondria are the major source of energy in mammalian cells where the main events related to ATP generation, calcium homeostasis regulation and programmed cell death induction occur [146]. The mitochondrial dysfunction has been observed in several diseases such as cancer, Parkinson's, Alzeimer's and amyotrophic lateral sclerosis. Therefore inhibiting the mitochondrial pathways has been identified as a potential therapeutic strategy. Cell penetrating peptides, polymers and lipophilic cationic conjugates have been shown to target mitochondria in order to trigger cell death in target tissues. *N*-(2-

hydroxypropyl)methacrylamide (HPMA) polymer conjugates were synthesized to deliver FITC to mitochondria *in vitro* [147]. Mitochondria-targeted biodegradable PLGA NPs have been fabricated for the treatment of a variety of diseases. PLGA was conjugated to PEG and triphenylphosphonium polymer (PLGA-*b*-PEG-TPP) [148]. The mitochondria targeting drugs, lonidamine and α-tocopheryl succinate were encapsulated for cancer, curcumin for Alzheimer's disease and 2,4-dinitrophenol (2,4-DNP) for obesity. When HeLa cells were treated with these NPs the efficiency of the drugs was 100 times higher than the drugs alone and five times higher than the non-targeted NPs. The curcumin entrapped NPs recovered almost 100% of the plaque-forming IMR-32 neuroblastoma cells compared 67% and 70% recovery of cells treated by free curcumin and non-targeted NPs, respectively. A mitochondria specific nanocarrier system was prepared using amphiphilic quinolinium derivative dequalinium chloride to induce pro-apoptotic actions in the mitochondria [149]. Dequalinium chloride was seen to accumulate selectively in the mitochondria of colo 205 cancer cells and trigger apoptosis.

Nuclear delivery

Nuclear localization is the most formidable challenge to the intracellular localization due to restricted diffusion through the nuclear pore complexes (NPC) at nuclear membrane [150]. Only small NPs less than 50 kDa (~10 nm) can enter the nucleus via passive diffusion, whereas macromolecules of size greater than 50 kDa may enter *via* active transport mediated by conjugating with NLS (PKKKRKV) sequence [8, 151]. The nuclear entry of plasmid DNA is thought to occur following DNA unpacking from polymer complexes [152]. Polyethylene imine (PEI) polymer conjugated with single or multiple NLS effectively transported plasmid DNA into the nucleus [153]. PEG-*b*-PCL micelles conjugated with NLS sequence and HER2 protein showed significant uptake and nuclear targeting in BT-474 or MDA-MB-231 cells [154]. Nucleic acid containing liposomes were used in combination with microbubbles to deliver luciferease gene or EGP siRNA to melanoma and hepatoma cells, respectively [155]. Another strategy is to dilate the NPCs using an amphipathic alcohol, *trans*-cyclohexane-1,2-diol (TCHD) in order to facilitate nuclear entry of plasmid DNA [156]. Nuclear delivery is also cell cycle dependent. Highest delivery to nuclear delivery has been found during the mitotic phase when nuclear envelope breaks down completely for cytoplasmic segregation of intracellular compounds into the daughter cells [157]. A lipid based silica NP with honeycombed porosity has been synthesized to store large amounts of drugs inside the pores [158]. The NPs were shown to deliver DOX specifically to human liver cancer cells due to high affinity of histidine rich fusogenic SP94 targeting peptides to the surface receptors. The NPs were released in the cytoplasm by osmotic swelling and membrane destabilization of endosomes by the protonation of imidazole groups of the fusogenic peptide. The peptides were also conjugated with NLS that enables nuclear delivery of not only DOX, but also other small molecules such as calcein and dsDNA. A pH responsive polymer poly((2-pyridin-2-yldisulfanyl)ethyl acrylate) (PDS) was synthesized by conjugating PEG, cRGD peptide for selective targeting and DOX drug [159].

Delivery to lysosomes

NPs after being internalized in endosomes may mature to lysosomes where the structures may be disintegrated into smaller molecules by the proteolytic degradation in an acidic environment at pH 4.5. PLGA NPs colocalize in lysosomes after a few minutes of incubation with human arterial smooth muscle cells (HASMCS) [160]. The lysosomal localization of anti-ICAM conjugated NPs was delayed in HUVEC cells by pretreating the cells with a lysosomal enzyme activity suppressor, chloroquine or the microtubule stabilizing drug, nocodazole [161]. Chloroquine or nocodazole treatment delayed the lysosomal degradation of anti-ICAM NPs. In contrast to the lysosome avoiding pathway, some drug delivery systems function within the lysosomes. Poly(β-aminoester) ketal-2 polymer undergoes lysosomal degradation in order to increase the cytoplasmic delivery of the drug [162]. The polymer was used to encapsulate Cy-5 labeled enhanced green fluorescent protein (EGFP) DNA to transfect HCT116 colon cancer cells. The flow cytometry analysis showed increasing Cy-5 DNA positive cells and three fold higher EGFP expression compared to the PLGA NPs. The low endosomal pH was inhibited by inhibition of V-ATPases using bafilomycin A1 that decreased the EGFP expression significantly indicating the activity of the polymer in acidic pH. PLGA NPs were conjugated with anti-cytokeratin monoclonal IgG to deliver a potent protease inhibitor, cystatin to breast cancer cells in order to inhibit the proteolytic activity [163]. Using fluorescence microscopy and flow cytometry, it has been shown that cystatin delivered with the targeted NPs had higher potential in inhibiting intracellular proteolytic activity than free cystatin that was unable to enter the cells. These methods are important for avoiding drug degradation in lysosomes. However, some NPs are activated after exposure to the lysosomal low pH and high enzymatic conditions. For example, a targeted pH sensitive micelle NP, $(PEO)_{129}(P2VP)_{43}(PCL)_{17}$ABC induced protonation at low pH (~5) that released 3.5 fold more of the encapsulated dye (Nile Red) than the unprotonated micelle control after 4 h incubation in gliosarcoma cells [164]. HPMA copolymer conjugates containing DOX exhibited lysosomal entry where the tetrapeptidyl Gly-Phe-Leu-Gly drug linker is cleaved by lysosomal thiol dependent proteases, particularly cathepsin B [165]. The HPMA copolymer-DOX conjugates demonstrated higher MTD and anti-cancer activity in MCF-7 breast cancer cells *in vitro* and in many *in vivo* models than DOX alone [166]. The polymer-drug conjugates entered phase I/II clinical trials for the treatment of breast, lung and colon cancers [12].

PENETRATION OF NPs ACROSS SKIN

Skin structure and diffusion limitations

Skin is the largest organ of the body with a surface area of about 1.2–1.3 m^2 and a thickness less than 2 mm [167]. It consists of three layers: the epidermis, dermis and hypodermis. For details, see Ref. [168]. The topmost sub-layer of epidermis, *stratum corneum*poses a rate limiting barrier for diffusion. *Stratum corneum* is composed of lipids including ceramides, triglycerides, cholesterols and free fatty acids. The dermis layer is composed of elastin and collagen fibers that provide mechanical support of skin. It is highly vascularized and permeable to solutes. Appendages such as hair follicles, sebaceous glands and sweat glands

are also found in this layer. All these layers provide a defensive barrier to the external environment

Recent literature on NP penetration

The rate limiting step during transdermal transport of drugs is permeation across the *stratum corneum* [169, 170]. Several methods have been designed to enhance transdermal drug delivery by using permeation enhancers or by disrupting the epidermis using physical means such as sonophoresis, electroporation and microneedles [171, 172]. Several of these methods have been shown to enhance topical delivery of NPs [13, 173–175]. However, these methods rely on inducing structural changes in skin and are not discussed here. These methods are discussed in depth elsewhere [176, 177]. Below, we summarize reports of delivering NPs across the skin that do not rely on obvious disruption of the skin structure.

Liposomes, ethosomes and transferosomes

Penetration of liposomes across the skin been studied, although the precise mechanisms by which they penetrate the skin are not clear. It is generally accepted that liposomes do not penetrate the vesicles as intact vesicles [168, 178]. Liposomes can fuse with the lipids in the *stratum corneum*. Alternatively, liposomes can disintegrate on the skin surface where the lipid molecules can enter the *stratum corneum* by disrupting the packing and fluidity of the lipid bilayers. Liposomes could also enter the sebaceous glands and act as a drug reservoir. Liposomes have been used for acne, psoriasis, infections and other skin diseases [179]. Ethosomes are lipid- or surfactant-based vesicles forming with, ethanol [180]. Drugs encapsulated in ethosomes have been reported for deep skin penetration and systemic absorption. The inclusion of a high level (~30%) of ethanol in the phospholipid structure creates not only a flexible bilayer but also allow deposition followed by breaking of the *stratum corneum* bilayers. Several drugs have been delivered into skin using ethosomes [180–185]. Transfersomes are deformable liposomes that are composed of phospholipids and surfactants *e.g.* sodium deoxycholate, Span 80 and Tween 80 to destabilize the lipid bilayers [186]. They have also been shown to deliver drugs for the topical treatment of psoriasis and acne, among others [187].

Solid Lipid NPs (SLNs)

SLNs are a blend of solid lipids (0.1 to 30% w/w) dispersed in an aqueous medium with stabilizing surfactants (0.5 to 5% w/w) [188]. SLNs have been used for the treatment of atopic eczema, acne, psoriasis and rheumatoid arthritis. Recently SLN gel has been developed to deliver meoxicam (MLX) drug using the microemulsion technique [189]. MLX penetration was *tested in vitro* in rat skin using the Franz diffusion cell. Tretinoin was delivered using SLNs to improve its efficacy for the treatment of psoriasis without causing side effects. SLNs offered enhanced photostability, increased skin transport and anti-psoriatic activity compared to the commercial liposomes in mice skin [185]. SLNs have also been used to deliver isotretinoin [190].

Polymeric NPs

Both synthetic and natural polymers have been used for drug delivery into the skin [191]. The most widely used polymers are poly(ε-caprolactone) (PCL), poly(methyl methacrylate), PLA, poly(glycolic acid), and their co-derivatives PLGA [192, 193]. These polymers are biocompatible and biodegradable. Polymeric NPs are usually found to accumulate in the hair follicles that act as a long term reservoir to release drugs in the *stratum corneum*. Curcumin encapsulated with poly(vinyl alcohol) polymers was shown to penetrate deep into the hair follicles of pig skin [194]. Chitosan-coated PLGA NPs have also been used for the transfollicular delivery of ovalbumin (OVA) in pig skin [195]. The immunization capacity of OVA or diphtheria toxoid (DT) loaded *N*-trimethyl chitosan (TMC) polymer has been tested in mice skin [196]. OVA-TMC NPs enhanced the anti-OVA IgG titers in the sera of mice after sub-cutaneous injection. DT-TMC induced 200-fold higher titers of anti-DT IgG levels after the first immunization than those after DT injection alone.

Lipid-polymer hybrid NPs (CyLiPn) have been designed using a PLGA core, PEG shell, cyclic pyrrolidinium head group and DOPC monolayer to deliver anti-TNFα siRNA (siTNFα) for the treatment of chronic skin inflammatory disease [175]. CyLipN siRNA penetrated deeper (360 μm) into the dermal region than the control at a depth of 280 μm. For the treatment of psoratic skin lesions, siTNFα delivery using CyLipn showed faster and complete healing than the control siTNFα carriers at the end of 5 day treatment. The histological sectioning of skin treated with siTNFα-CyLipn showed normal skin behavior where the untreated skin showed increased epidermal thickening with elongated epidermal ridges in both dermis and epidermis.

Peptides

Transdermal delivery of peptides is limited by the *stratum corneum*. A number of cell-penetrating peptides have been found to cross the skin may be due to the content of positively charged arginine or lysine residues [197, 198]. Recently, a skin penetrating and cell entering (SPACE) peptide (AC-TGSTQHQ-CG) was found to penetrate into a number of cultured cells including keratinocytes and fibroblasts as these cells are found in the *stratum corneum* (Fig. 8a) [199]. A space-ethosome NP system enhanced the delivery of a hydrophilic dipolysaccharide, hyaluronic acid (HA) by ~7.8 fold compared to the vehicle free HA delivery in PBS into skin *in vitro* (Fig. 8b) [200]. The *in vivo* experiments showed 5-fold higher HA deposition in the dermal layer than that using PBS. The HA concentration was 1000-fold higher in the local skin tissue under the application site than those tested in the blood. The same system was also shown to enhance skin penetration of siRNA-lipid nanocomplexes.

NP PERMEATION ACROSS MUCOSAL BARRIERS

Mucus serves to exclude pathogens and other dangerous materials from the underlying cells allowing the diffusion of only nutrients, proteins and essential molecules [201]. It is the primary defense mechanism of mucosal tissues in order to efficiently trap and remove nano- and micro-sized objects, viruses and bacteria. However, pathogens have developed strategies to effectively penetrate the mucus layer by excreting the mucolytic agents such as mucinases

and sialidases. For example, influenza viruses utilize neuraminidase protein to cleave sialic acid groups on the mucus layer, thus allowing penetration of the mucosal barrier [202].

Mucosal surfaces protect all major portals of our body such as nose, lung, intestine, gall bladder, urinary bladder and reproductive tracts [201]. The mucus layer is composed of mainly water (90–98%), mucin proteins (2–5%) including glycoproteins, lipids and mineral salts. Mucins are highly glycosylated proteins forming a viscoelastic gel network that is 1000–10,000 times more viscous than water at low shear rates [203]. It is negatively charged due to the presence of sialic acid and sulfated monosaccharides in the sugar chains. The thickness of the mucus layer varies from 5 μm in the eye, to 300 μm in the stomach and 700 μm in the intestine. The characteristic pore size of diffusion channels in the mucus is ~20–200 nm [204]. However, abnormal mucus has been found in several diseases including asthma, cystic fibrosis, lung cancer and ocular diseases. Recent studies using NPs have shown that NP size up to hundreds of nanometers can diffuse through the mucus in a few minutes (Fig. 9) [205–208]. The epithelium beneath the mucus layer consists of a layer of epithelial cells that are closely stacked together by tight junctions. The gaps between the tight junctions are less than 0.1 nm restricting the delivery of NPs.

There are mainly two mechanisms by which NPs can cross the epithelial cells under the mucus layer: the paracellular and transcellular pathways [209]. Paracellular transport pass substances through intercellular spaces between epithelial cells *via* diffusion. Transcellular transport occurs directly across the epithelial cells. The two most abundant epithelial cells are absorptive (enterocytes) and secretory cells (goblet and Paneth). Goblet cells secrete mucin. In addition to the aforementioned cells, there exist M cells in the Peyer's patches that lack the mucus layer, and contain fewer cytoplasmic lysosomes. NPs with size less than 50 nm are transported paracellularly, those with sizes between 50–200 nm are endocytosed by enterocytes, and those between 200 nm up to 5 μm are taken up by M cells of the Peyer's patches [210].

Penetration of NPs across the mucus

Mucus immobilizes particles by hydrophobic and electrostatic interactions as well as hydrogen bonding. Strategies to overcome this barrier are to design mucoadhesive particles, mucus penetrating particles and mucolytics [203]. The objectives of these studies have been to increase the absorption of drugs across the mucus, increase the residence time in the tightly packed mucus layer to delay its intestinal clearance and improve the diffusion across the mucus barrier. In the following sections, current strategies to overcome the biological barriers in the mucus layer are discussed.

A variety of biodegradable and biocompatible polymers e.g. PCL, PLA, PLGA, HA, poly(acrylic acid) (PAA), poloxamers, polyethylene oxide (PEO), polyglutamic acid, chitosan, alginate, lipids, liposomes and hydrogels have been used for enhanced drug permeability and extended drug release in the mucosal surface [211]. Size-dependent absorption mechanisms of polystyrene particles have been investigated using 300, 600 and 1000 nm particles [212]. Smaller (300 nm) particles demonstrated higher levels in intestinal transport *in vivo via* enterocytes and M cells than the larger particles. Negatively charged NPs of ~ 200–500 nm showed higher diffusion coefficients than smaller (~25–50 nm)

particles [206, 213, 214]. Many NPs are designed to dissociate at acidic pH where the pH in the mucus layer of small intestine (pH ~6) and vagina is acidic (pH 3.5–4.5) [203]. NPs may also cause alteration of the microstructure of human mucus thus offering an unique approach to enhance drug and gene delivery to mucosal surfaces [215].

Incorporation of PEG into NPs is known to decrease the interactions with other proteins and biomacromolecules [216]. PEG-PLGA has been shown to move two-fold (~5.9 mm/min) faster than the PLGA alone or PVA grafted PLGA (2.6 mm/min) [217]. In a separate study, diffusion of PEG-PLGA NPs was found 3–10 fold higher than unmodified PLGA [218]. The mean squared displacement (MSD) of PEG-polysebacic acid (PSA) was 400 and 230-fold higher than that of PSA or PLGA, respectively in human cervicovaginal mucus (CVM) [207]. PEG conjugation to carboxyl functionalized polystyrene particles increased the diffusion of larger NPs (200 and 500 nm) than smaller (100 nm) NPs in CVM [206]. High PEG density using a short chain (2 kDa) showed better mucus penetration of NPs than that of a heavy chain (10 kDa) PEG [219]. This effect was due to muco-inertness of NPs by shielding the NP surface using short chain PEG, resulting in little NP interactions with mucin fibers. A reduction of 40% PEG surface coverage decreased NP transport by 700 fold in human mucus [219]. Anionic poly(amido amine) (PAMAM) dendrimer (generation G3.5) while PEGylated showed a considerable increase in cellular uptake and high drug transport compared to PEGylated G4.5 dendrimers [220].

The linker chemistry determines the stability and efficacy of drug conjugates. Glycine linker in the G3.5-Glycine-SN38 drug conjugates showed higher stability and efficacy than Alanine linker in G3.5-Alanine-drug conjugates [220]. In recent years, mucoadhesive materials such as chitosan, PLA, PLGA, poly(sebacic acid) and PAA have been tested that adhere to the mucus layer [215, 221]. An alternative approach to overcome the mucus barrier is to remove the mucus surface improving absorption [207], however this method increases the risk of bacterial contamination in epithelial cells [222]. Understanding these factors gives an opportunity to develop safe and more effective NPs for oral therapeutic delivery.

Penetration of NPs across epithelium

Oral/Intestine—Oral administration is the most widely used method of delivering drugs. The key challenges of oral drug delivery are the poor drug solubility, stability in variable pHs of biological environment in the gastrointestinal (GI) tract, a protective mucus layer and presence of digestive enzymes [209, 223]. Therefore, delivery through the oral route requires innovative design and formulation of a drug delivery system for better bioavailability and biodistribution. For example, insulin-loaded NPs have conserved insulin activity and decreased blood glucose level as well as oral bioavailability in diabetic rats for up to 14 days following the oral delivery [210, 224, 225]. Natural hydrogels such as dextran, chitosan, alginate and gelatin have been tested for nanoparticulate oral drug delivery [167]. Micellar polymeric NPs consisting of PLA, PCL and PEO have shown enhanced uptake and controlled drug release at the absorption site [226].

To prolong NP residence time at the absorption site, mucoadhesive polymers are used for enhancing interactions with mucus. The possible mechanisms of interactions are hydrogen

bonding, hydrophobic, electrostatic or van der Waals interactions [227]. The most exploited forms of mucoadhesive NPs are chitosan, gelatin, PAA, PEI, poly-l-lysine (PLL) and PAMAM dendrimers [227]. Besides absorption, other transport mechanisms for oral drug delivery are paracellular pathway, or transcellular mechanism *via* clathrin- and caveolae-dependent endocytosis. PAMAM dendrimers were found to transport across Caco-2 cell monolayers by a combination of paracellular pathway and transcellular endocytosis [228, 229]. Penetration of the NPs can be further enhanced by surface modification using a penetration enhancer (e.g., lauric acid) compared to unmodified dendrimers [230].

After oral administration, the common absorption site of NPs is the small intestine. The major cell types in the small intestine are absorptive enterocytes, mucus secretory goblet cells and the immune sampling microfold cells (M-cells) [231]. The M cells are associated with lymphocytes, immunoblasts, plasma cells and macrophages. NPs are taken up by M cells and the intestinal enterocytes, There are a number of studies to investigate the uptake, translocation and biodistribution of NPs both *in vitro* intestine-like mammalian cell lines, including human adenocarcinoma Caco-2 cells, mucus-secreting MTX-E12 cells and in the small intestine in the body. PTX delivered with lipid nanocapsules for intestinal delivery showed higher permeability of the drug than Taxol [232]. Later, it has been shown that modified characteristics of NP surface offers higher penetration through the mucus. Chitosan NPs with pluronic F127 lipid shell and PEO corona exhibited higher efficiency in mucosal penetration when delivering insulin to rat intestine [225]. Porous silicon NPs conjugated with a hydrophilic peptide (YY3-36) penetrated the Caco-2 monolayer colon cancer cells in the co-culture with HT-29 mucus producing cells [233]. YY3-36 is a high molecular weight human peptide, tyrosine tyrosine 3–36 consisting of 36 amino acids [233]. When loaded with silicon NPs, YY3–36 facilitates permeation across the Caco-2 monolayers. Similar study was carried out using PEG2000 conjugated SLNs (pSLN) for the delivery of DOX to Caco-2 cells in the co-culture of Caco-2/HT29 monolayers [234]. The permeability coefficient P_{app} was measured 1.5–2 fold greater for pSLNs than that using SLNs in the three different regions of intestine. *In vivo* pharmacokinetics data showed that the relative bioavailability of pSLN-DOX was 1.99 to 7.5 fold higher than SLN-DOX indicating higher penetration and longer retention of pSLN-DOX in the intestine while the unmodified SLNs were trapped and cleared out of the mucosal tissue. PLGA NPs conjugated with lectin peptide were detected 1.4–3.1 fold higher than the unconjugated NPs in the small intestine suggesting an increase in intestinal bioadhesion and endocytosis [235]. A pH responsive chitosan and poly(γ-glutamic acid) NP system has also been designed for the oral delivery of insulin in order to open the tight junctions between the epithelial cells [224, 236]. The dilation of the intercellular space using chitosan was reversible without causing any cytotoxic effects. A targeting peptide (CSKSSDYQC) coated chitosan has been shown to enhance penetration of insulin across the epithelium [237]. The CSK peptide is a potent goblet cell targeting agent of intestinal epithelial cells offering a promise for intestinal drug delivery. Recent studies have also shown enhanced uptake of NPs across the intestine using targeting the Fc receptor [238].

Lung—A lot of inhaled materials is trapped in the respiratory mucus that lines the respiratory epithelium from the nose to the terminal bronchioles [239]. In human lungs, the

mucus layer is composed of two distinct layers: the periciliary (sol) layer (~5–10μm thick) and the luminal (gel) layer (~60μm thick). The sol layer is watery, less viscous and close to the epithelium. The gel layer contains cilia to propel mucus up and out of the lung functioning to trap any external material for delivery. Strategies to overcome this barrier include mucoadhesive, mucus penetrating and mucolytics particles. Traditional hydrophobic particles such as PLGA, PLA and PCL are adhesively trapped in mucus, whereas neutral and hydrophilic particles may decrease the adhesion to the mucus fibers. Peptide bunches on nanocage (PBNC) conjugated with cysteine containing AP-1 (cysAP1) peptide (RKRLDRN) showed enhanced avidity to the interleukin-4 receptor (IL-4) in A549 lung cancer cells [240]. More specifically, one peptide with cysteine at 157 position, ^{157}cysAP-1 promotes the association with its target, IL-4 receptor diminishing the symptoms of allergic asthma *in vivo* [240]. Chemotherapeutic drugs delivered through the pulmonary route can be concentrated in the lungs and surrounding lymph nodes. A liposomal formulation of 9-nitro-camptothecin (9-NC) and a vitamin E analog (α-TEA) inhibited the growth of lung cancer and lymph node metastases to a greater extent than 9-NC treatment alone [241]. Delivery of drugs to the lungs is a non-invasive method for systemic exposure over intravenous injection. Insulin release in the systemic circulation from the lungs showed a significant reduction in blood glucose level with a long time effect over 20–48 h compared to insulin solution [242–244]. Large (~10μm) porous estradiol particles showed 1.5–4.7 fold more bioavailability than smaller particles (~3μm) by enhancing the retention time (96 h) in lungs. Combination treatment of rifampicin, isoniazid and pyrazinamide as delivered with solid lipid NPs (SLNs) showed slow and sustained release of the drugs for the treatment of tuberculosis both *in vitro* and *in vivo* [245]. The systemic administration of drugs through lungs offers an effective means of drug delivery.

Nose—The local and systemic delivery of drugs through the nasal route is non-invasive, painless and easily accessible route allowing a high rate of drug absorption [246]. The nasal cavity is comprised of anterior and posterior vestibules, an atrium, an olfactory region, the nasopharynx and a respiratory area. It also has the glandular epithelium cells that secrete the mucus layer. To design a drug delivery system through the nasal mucosa, it has to overcome two main barriers: the mucus layer and the endothelium. The combination treatment of insulin-loaded chitosan NPs and a mucolytic agent, acetyl cysteine enhanced the nasal delivery of insulin in rats compared to the chitosan-mediated delivery [192]. More examples of recent advances in nasal drug delivery can be found in Refs. [246, 247].

Vagina—The vaginal mucus consists of 95% water, 1–2% mucin fibers and trace amounts of lactic acid, lipids, salts, proteins and enzymes [248]. The mucin fibers form a viscoelastic gel by crosslinking the fibers in water that limits the drug penetration across the vaginal tract. A variety of drugs such as antifungals, spermicides, contraceptive hormone and agents facilitating ovulation or abortion have been targeted to the vagina. PEG-coated polystyrene particles of different sizes (200, 500 and 1000 nm) were used to probe the microstructure of human cervicovaginal mucus (CVM) at various pHs (1–2, 4, 6–7 and 8–9) [208]. The pore size of CVM as measured from the particle motion (~370 nm at pH 4) decreased with increasing pH (~210 nm at pH 8–9). The viscoelasticity of CVM decreased by 2-fold from pH 4 to 8–9. The NPs of 100 nm size showed long term retention and protection in the

vagina [205]. Gene delivery vectors using PEG, cystamine core poly(amido amine) (PAMAM S-S) and PEI (25kDa) conjugated dendrimers were developed for efficient delivery to mucosal surfaces of a variety of diseases [249]. There have been a few studies that used CPPs for siRNA intravaginal transfection in order to penetrate the CVM and reach the target cells [248].

SUMMARY AND FUTURE PERSPECTIVES

This review provides an overview of the advances in nanotechnologies being made towards overcoming the biological barriers. To encounter these barriers, a vast range of NPs have been developed that include synthetic polymeric carriers (e.g. polymeric NPs, polymer-drug conjugates, micelles and dendrimers), natural polymers, stimuli (e.g. pH, temperature and enzyme) responsive polymers, liposomes, SLNs, drug NPs, drug emulsions, peptides, porous structures and shape specific NPs. The NPs have been designed both for diagnostic and treatment enabling their transport across the barriers *i.e.* endothelium, skin and mucus layer.

The EPR effect of the defective endothelium leaks out NPs into the surrounding tissues causing the accumulation of NPs at the disease site. It is commonly seen in tumor and atherosclerosis. Although EPR effect is advantageous for the accumulation of both passive or active targeting NPs, further improvements are necessary to enhance the extravasation and movement of NPs from the blood vessels into the tumor cells. This can be accomplished by enhancing diffusion into dense tissue microenvironment, altering the IFP of tumor vasculatures and inducing the cancer cell apoptosis, simultaneously. Multifunctional NPs with optimum design parameters (e.g. size, shape, surface, compositions and physico-chemical properties) and aiming at multiple targets may address these challenges to improve the EPR effect based drug delivery.

The BBB is another formidable hurdle for NP delivery. TfR and IR receptor targeting ligands and some peptides have been used for the transport of NPs into the brain. Cell-mediated drug delivery suggest unloading of therapeutic agents at the disease site. However, the design of a highly efficient BBB shuttle is the most challenging issue in drug development.

Accordingly, advanced *in vitro* systems are necessary to visualize/image the penetration of NPs across endothelium. *In vivo* experiments are limited by confounding factors and lack of direct visual access to the endothelium. Transwell assays are available in which NPs are flown over cultured cells mimicking the *in vivo* environment of microcirculation. Another approach is to grow cells within the ECM gels to develop 3D cell culture models in order to mimic the function of tissue-tissue interfaces between epithelium and vascular endothelium. This enables the researchers not only to visualize the drugs but also provide a quantitative understanding of the transport parameters such as effective diffusion coefficient. Parallel-plate flow chambers have been used to study endothelial cell responses to hydrodynamic forces [250].

Microfluidic devices have been developed using PDMS substrate containing microchannels in order to create microenvironments for cultured cells. The cellular behavior is indeed quite

sensitive to the biological microenvironments in 3D structures for a variety of clinical applications [251–254]. Such approaches are useful to mimic tumors in microfluidics environment, model tumor-vascular interface [255], investigate tumor cell migration dynamics (Fig. 10), or investigate the role of fluid shear stress on tumor endothelial cells and mimic the BBB for better understanding of physiological microcirculatory environment of the brain [256].

Penetration of NPs across the skin and mucosal membranes warrants further investigations. In particular, polymeric NPs have not been studied in this context compared to the lipid-based. Stability of lipid based NPs is one of the concerns for topically delivering drugs. Needle-free administration of NPs has generated significant interest to enhance the transmucosal delivery of macromoleucles through the mucosal surface. Despite major advancements, there is still significant work ahead for many NPs to be developed into clinical use with high therapeutic efficacy, detailed biodistribution analysis and pharmacokinetics. Detailed physicochemical characterizations are necessary to understand the final products of the NPs and their clinical determinants in the human body. Future research should take these considerations into account.

Acknowledgments

This work was supported by the National Institute of Health under Grant No. R01DK097379.

Biographies

Dr. Sutapa Barua is a postdoctoral scholar in Professor Samir Mitragotri’s laboratory in Department of Chemical Engineering at University of California, Santa Barbara. She graduated from Arizona State University, Tempe in 2011 and earned a Ph.D. degree in Chemical Engineering. She works on nanoparticle design, drug delivery and cancer cells. Her research interests are in developing shape-specific drug nanoparticles for efficient interactions with the cell membrane, and inducing growth inhibition of malfunctioning cancer cells.

Professor Samir Mitragotri is Duncan and Suzanne Mellichamp Chair of Systems Biology and Bioengineering and Professor of Chemcial Engineering at the Univesity of California, Santa Barbara (UCSB). He also serves as the founding director of UCSB’s Center for

Bioengineering and director of UCSB's Translational Medical Research Laboratories. He received Ph.D. from MIT in 1996 and B.S. from Institute of Chemical Technology, Mumbai in 1992. Prof. Mitragotri's research interests are in the field of drug delivery and biomaterials. He is an elected fellow of National Academy of Inventors, American Association of Advancement of Science and American Institute of Medical and Biological Engineering.

REFERENCES

1. Yoo JW, Chambers E, Mitragotri S. Curr. Pharm. Des. 2010; 16:2298. [PubMed: 20618151]
2. Galley HF, Webster NR. Br. J. Anaesth. 2004; 93:105. [PubMed: 15121728]
3. Jain RK. Cancer Res. 1987; 47:3039. [PubMed: 3555767]
4. Jain RK, Baxter LT. Cancer Res. 1988; 48:7022. [PubMed: 3191477]
5. Rakesh KJ, Triantafyllos S. Nat. Rev. Clin. Oncol. 2010; 7:653. [PubMed: 20838415]
6. Netti PA, Berk DA, Swartz MA, Grodzinsky AJ, Jain RK. Cancer Res. 2000; 60:2497. [PubMed: 10811131]
7. Bareford LM, Swaan PW. Adv. Drug Delivery Rev. 2007; 59:748.
8. Macara IG. Microbiol. Mol. Biol. Rev. 2001; 65:570. [PubMed: 11729264]
9. Working PK, Newman MS, Huang SK, Mayhew E, Vaage J, Lasic DD. J. Liposome Res. 1994; 4:667.
10. Mark ED, Jonathan EZ, Chung Hang JC, David S, Anthony T, Christopher AA, et al. Nature. 2010; 464:1067. [PubMed: 20305636]
11. Gordon AN, Fleagle JT, Guthrie D, Parkin DE, Gore ME, Lacave AJ. J. Clin. Oncol. 2001; 19:3312. [PubMed: 11454878]
12. Seymour LW, Ferry DR, Kerr DJ, Rea D, Whitlock M, Poyner R, et al. Int. J. Oncol. 2009; 34:1629. [PubMed: 19424581]
13. Ying-Chen C, Der-Zen L, Jun-Jen L, Tsung-Wei C, Hsiu OH, Ming-Thau S. Int. J. Nanomedicine. 2012; 7
14. Nugent, G. BIND Doses First Patient in a Phase 2 Clinical Study of BIND-014 in Prostate Cancer. Cambridge, MA: 2013.
15. Amoozgar Z, Yeo Y. Wiley Interdiscip. Rev. Nanomed. Nanobiotechnol. 2012; 4:219. [PubMed: 22231928]
16. Dobrovolskaia MA, Aggarwal P, Hall JB, McNeil SE. Mol. Pharm. 2008; 5:487. [PubMed: 18510338]
17. Félétou, M. The Endothelium. 1st ed.. San Rafael: Morgan & Claypool Life Sciences; 2011.
18. Aird WC. Circ. Res. 2007; 100:158. [PubMed: 17272818]
19. Wong A, Ye M, Levy A, Rothstein J, Bergles D, Searson PC. Front. Neuroeng. 2013; 6
20. Stan, R. Cell-Cell Channels. Frantisek Baluska, DV.; Barlow, Peter W., editors. New York: Springer; 2006. p. 251-266.
21. Nies AT. Cancer Lett. 2007; 254:11. [PubMed: 17275180]
22. Dean M, Rzhetsky A, Allikmets R. Genome Res. 2001; 11:1156. [PubMed: 11435397]
23. Hobbs SK, Monsky WL, Yuan F, Roberts WG, Griffith L, Torchilin VP, et al. Proc. Natl. Acad. Sci. U.S.A. 1998; 95:4607. [PubMed: 9539785]
24. Hashizume H, Baluk P, Morikawa S, McLean JW, Thurston G, Roberge S, et al. Am. J. Path. 2000; 156:1363. [PubMed: 10751361]
25. Rowinsky EK, Donehower RC. N. Engl. J. Med. 1995; 332:1004. [PubMed: 7885406]
26. Ringel I, Horwitz SB. J. Natl. Cancer Inst. 1991; 83:288. [PubMed: 1671606]
27. Gradishar WJ, Tjulandin S, Davidson N, Shaw H, Desai N, Bhar P, et al. J. Clin. Oncol. 2005; 23:7794. [PubMed: 16172456]

28. Paz-Ares L, Ross H, Brien MO, Riviere A, Gatzemeier U, Pawel JV, et al. Br. J. Cancer. 2008; 98:1608. [PubMed: 18475293]
29. Christopeit M, Lenz G, Forstpointner R, Bartelheim K, Kühnbach R, Naujoks K, et al. Chemotherapy. 2008; 54:309. [PubMed: 18701819]
30. Yuan F, Dellian M, Fukumura D, Leunig M, Berk DA, Torchilin VP, et al. Cancer Res. 1995; 55:3752. [PubMed: 7641188]
31. Gabizon A, Catane R, Uziely B, Kaufman B, Safra T, Cohen R, et al. Cancer Res. 1994; 54:987. [PubMed: 8313389]
32. Symon Z, Peyser A, Tzemach D, Lyass O, Sucher E, Shezen E, et al. Cancer. 1999; 86:72. [PubMed: 10391566]
33. Ruth D. Nat. Rev. Cancer. 2006; 6:688. [PubMed: 16900224]
34. Moulton KS, Olsen BR, Sonn S, Fukai N, Zurakowski D, Zeng X. Circulation. 2004; 110:1330. [PubMed: 15313955]
35. Bazzoni G, Estrada OMMn, Dejana E. Trends Cardiovasc. Med. 1999; 9:147. [PubMed: 10639719]
36. Fuster V. Circulation. 1994; 90:2126. [PubMed: 7718033]
37. Joner M, Morimoto K, Kasukawa H, Steigerwald K, Merl S, Nakazawa G, et al. Arteriosclerosis, Thrombosis, and Vascular Biology. 2008; 28:1960.
38. Song C, Labhasetwar V, Cui X, Underwood T, Levy RJ. J. Controlled Release. 1998; 54:201.
39. Ikuta K, Mori T, Yamamoto T, Niidome T, Shimokawa H, Katayama Y. Bioorg. Med. Chem. 2008; 16:2811. [PubMed: 18226910]
40. Uwatoku T, Shimokawa H, Abe K, Matsumoto Y, Hattori T, Oi K, et al. Circ. Res. 2003; 92:e62. [PubMed: 12663484]
41. Akagi D, Oba M, Koyama H, Nishiyama N, Fukushima S, Miyata T, et al. Gene Ther. 2007; 14:1029. [PubMed: 17460721]
42. Chan JM, Zhang L, Tong R, Ghosh D, Gao W, Liao G, et al. Proc. Natl. Acad. Sci. U.S.A. 2010
43. Mulder WJM, Douma K, Koning GA, van Zandvoort MA, Lutgens E, Daemen MJ, et al. Magnetic Resonance in Medicine. 2006; 55:1170. [PubMed: 16598732]
44. Sirol M, Itskovich VV, Mani V, Aguinaldo JGS, Fallon JT, Misselwitz B, et al. Circulation. 2004; 109:2890. [PubMed: 15184290]
45. Amirbekian V, Lipinski MJ, Briley-Saebo KC, Amirbekian S, Aguinaldo JGS, Weinreb DB, et al. Proc. Natl. Acad. Sci. U.S.A. 2007; 104:961. [PubMed: 17215360]
46. McCarthy JR, Korngold E, Weissleder R, Jaffer FA. Small. 2010; 6:2041. [PubMed: 20721949]
47. Cormode DP, Skajaa T, van Schooneveld MM, Koole R, Jarzyna P, Lobatto ME, et al. Nano Lett. 2008; 8:3715. [PubMed: 18939808]
48. Skajaa T, Zhao Y, van den Heuvel DJ, Gerritsen HC, Cormode DP, Koole R, et al. Nano Lett. 2010; 10:5131. [PubMed: 21087054]
49. Hrkach J, Von Hoff D, Ali MM, Andrianova E, Auer J, Campbell T, et al. Sci. Transl. Med. 2012; 4:128ra39.
50. Chang SS, O'Keefe DS, Bacich DJ, Reuter VE, Heston WD, Gaudin PB. Clin Cancer Res. 1999; 5:2674. [PubMed: 10537328]
51. Vivek Mishra SM, Rawat Amit, Gupta Prem N, Dubey Praveen, Khatri Kapil, Vyas Suresh P. J. Drug Targeting. 2006; 14:45.
52. Davis ME. Mol. Pharm. 2009; 6:659. [PubMed: 19267452]
53. Choi CHJ, Alabi CA, Webster P, Davis ME. Proc. Natl. Acad. Sci. U.S.A. 2010; 107:1235. [PubMed: 20080552]
54. Winter PM, Caruthers SD, Zhang H, Williams TA, Wickline SA, Lanza GM. JACC Cardiovasc. Imaging. 2008; 1:624. [PubMed: 19356492]
55. Simone E, Ding BS, Muzykantov V. Cell and tissue research. 2009; 335:283. [PubMed: 18815813]
56. Pardridge WM. Adv. Drug Delivery Rev. 1995; 15:5.
57. Begley DJ. Pharmacol. Ther. 2004; 104:29. [PubMed: 15500907]

58. Aktaş Y, Yemisci M, Andrieux K, Gürsoy RN, Alonso MJ, Fernandez-Megia E, et al. Bioconjugate Chem. 2005; 16:1503.
59. Lee HJ, Engelhardt B, Lesley J, Bickel U, Pardridge WM. J. Pharmacol. Exp. Ther. 2000; 292:1048. [PubMed: 10688622]
60. Gaillard PJ, Visser CC, de Boer AG. Expert Opin. Drug Deliv. 2005; 2:299. [PubMed: 16296755]
61. Boado RJ, Zhang Y, Zhang Y, Pardridge WM. Biotechnol. Bioeng. 2007; 96:381. [PubMed: 16937408]
62. Ulbrich K, Knobloch T, Kreuter J. J. Drug Targeting. 2011; 19:125.
63. Schröder U, Sabel BA. Brain Res. 1996; 710:121. [PubMed: 8963650]
64. Gulyaev A, Gelperina S, Skidan I, Antropov A, Kivman G, Kreuter J. Pharm. Res. 1999; 16:1564. [PubMed: 10554098]
65. Ambruosi A, Khalansky AS, Yamamoto H, Gelperina SE, Begley DJ, Kreuter J. J. Drug Targeting. 2006; 14:97.
66. Alyautdin R, Petrov V, Langer K, Berthold A, Kharkevich D, Kreuter J. Pharm. Res. 1997; 14:325. [PubMed: 9098875]
67. Wong C, Stylianopoulos T, Cui J, Martin J, Chauhan VP, Jiang W, et al. Proc. Natl. Acad. Sci. U.S.A. 2011; 108:2426. [PubMed: 21245339]
68. Goodman TT, Olive PL, Pun SH. Int. J. Nanomedicine. 2007; 2:265. [PubMed: 17722554]
69. Champion JA, Katare YK, Mitragotri S. Proc. Natl. Acad. Sci. U.S.A. 2007; 104:11901. [PubMed: 17620615]
70. Agarwal R, Singh V, Jurney P, Shi L, Sreenivasan SV, Roy K. ACS Nano. 2012; 6:2524. [PubMed: 22385068]
71. Gratton SEA, Ropp PA, Pohlhaus PD, Luft JC, Madden VJ, Napier ME, et al. Proc. Natl. Acad. Sci. U.S.A. 2008; 105:11613. [PubMed: 18697944]
72. Perry JL, Reuter KG, Kai MP, Herlihy KP, Jones SW, Luft JC, et al. Nano Lett. 2012; 12:5304. [PubMed: 22920324]
73. Adriani G, de Tullio MD, Ferrari M, Hussain F, Pascazio G, Liu X, et al. Biomaterials. 2012; 33:5504. [PubMed: 22579236]
74. Godin B, Chiappini C, Srinivasan S, Alexander JF, Yokoi K, Ferrari M, et al. Adv. Funct. Mater. 2012; 22:4225. [PubMed: 23227000]
75. Barua S, Mitragotri S. ACS Nano. 2013; 7:9558. [PubMed: 24053162]
76. Barua S, Yoo J-W, Kolhar P, Wakankar A, Gokarn YR, Mitragotri S. Proc. Natl. Acad. Sci. U.S.A. 2013
77. Kolhar P, Anselmo AC, Gupta V, Pant K, Prabhakarpandian B, Ruoslahti E, et al. Proc. Natl. Acad. Sci. U.S.A. 2013; 110:10753. [PubMed: 23754411]
78. Huang X, Teng X, Chen D, Tang F, He J. Biomaterials. 2010; 31:438. [PubMed: 19800115]
79. Champion JA, Mitragotri S. Proc. Natl. Acad. Sci. U.S.A. 2006; 103:4930. [PubMed: 16549762]
80. Yan G, Paul D, Shenshen C, Richard T, Manorama T, Tamara M, et al. Nat. Nanotechnol. 2007; 2:249. [PubMed: 18654271]
81. Yu T, Hubbard D, Ray A, Ghandehari H. J. Controlled Release. 2012; 163:46.
82. Decuzzi P, Godin B, Tanaka T, Lee SY, Chiappini C, Liu X, et al. J. Controlled Release. 2010; 141:320.
83. Godin B, Chiappini C, Srinivasan S, Alexander JF, Yokoi K, Ferrari M, et al. Advanced Functional Materials. 2012; 22:4186.
84. Gentile F, Chiappini C, Fine D, Bhavane RC, Peluccio MS, Cheng MM-C, et al. J. Biomech. 2008; 41:2312. [PubMed: 18571181]
85. Decuzzi P, Ferrari M. Biomaterials. 2006; 27:5307. [PubMed: 16797691]
86. Grainger SJ, Serna JV, Sunny S, Zhou Y, Deng CX, El-Sayed MEH. Mol. Pharm. 2010; 7:2006. [PubMed: 20957996]
87. Watson KD, Lai C-Y, Qin S, Kruse DE, Lin Y-C, Seo JW, et al. Cancer Res. 2012; 72:1485. [PubMed: 22282664]
88. Caitlin WB, Eben A, Kelsie T, Alexander LK, Richard JP. Mol. Ther. 2013

89. Wei H, Huang J, Yang J, Zhang X, Lin L, Xue E, et al. PLoS ONE. 2013; 8:e58133. [PubMed: 23469265]
90. Liu H-L, Hua M-Y, Yang H-W, Huang C-Y, Chu P-C, Wu J-S, et al. Proc. Natl. Acad. Sci. U.S.A. 2010
91. Fan C-H, Ting C-Y, Lin H-J, Wang C-H, Liu H-L, Yen T-C, et al. Biomaterials. 2013; 34:3706. [PubMed: 23433776]
92. Etame AB, Diaz RJ, O'Reilly MA, Smith CA, Mainprize TG, Hynynen K, et al. Nanomed. Nanotechnol. Biol. Med. 2012; 8:1133.
93. Alessandro P, Nicoletta Q, Anne LvdV, Ciro C, Michael E, Jonathan OM, et al. Nat. Nanotechnol. 2012; 8:61. [PubMed: 23241654]
94. Chambers E, Mitragotri S. J. Controlled Release. 2004; 100:111.
95. Anselmo AC, Gupta V, Zern BJ, Pan D, Zakrewsky M, Muzykantov V, et al. ACS Nano. 2013; 7:11129. [PubMed: 24182189]
96. Doshi N, Zahr AS, Bhaskar S, Lahann J, Mitragotri S. Proc. Natl. Acad. Sci. U.S.A. 2009; 106:21495. [PubMed: 20018694]
97. Merkel TJ, Jones SW, Herlihy KP, Kersey FR, Shields AR, Napier M, et al. Proc. Natl. Acad. Sci. U.S.A. 2011
98. Kennedy L, Bear A, Young J, Lewinski N, Kim J, Foster A, et al. Nanoscale Res. Lett. 2011; 6:1.
99. Matthias TS, James JM, Soong Ho U, Anna B, Darrell JI. Nat. Med. 2010; 16:1035. [PubMed: 20711198]
100. Kolácná L, Bakesová J, Varga F, Kostáková E, Plánka L, Necas A, et al. Physiol. Res. 56 Suppl. 2007; 1:S51.
101. Levental KR, Yu H, Kass L, Lakins JN, Egeblad M, Erler JT, et al. Cell. 2009; 139:891. [PubMed: 19931152]
102. Jay SD, David AC. Nat. Rev. Cancer. 2010; 10:9. [PubMed: 20029421]
103. Baxter LT, Jain RK. Microvasc. Res. 1989; 37:77. [PubMed: 2646512]
104. Baxter LT, Jain RK. Microvasc. Res. 1991; 41:252. [PubMed: 2051960]
105. McKee TD, Grandi P, Mok W, Alexandrakis G, Insin N, Zimmer JP, et al. Cancer Res. 2006; 66:2509. [PubMed: 16510565]
106. Pluen A, Boucher Y, Ramanujan S, McKee TD, Gohongi T, di Tomaso E, et al. Proc. Natl. Acad. Sci. U.S.A. 2001; 98:4628. [PubMed: 11274375]
107. George A, Edward BB, Ricky TT, Trevor DM, Robert BC, Yves B, et al. Nat. Med. 2004; 10:203. [PubMed: 14716306]
108. Curti BD, Urba WJ, Gregory Alvord W, Janik JE, Smith JW, Madara K, et al. Cancer Res. 1993; 53:2204. [PubMed: 8485703]
109. Gregg LS. Nat. Rev. Cancer. 2003; 3:721. [PubMed: 13130303]
110. Rosa AC, Valeria C, Stephan JR. Nat. Rev. Cancer. 2005; 5:786. [PubMed: 16175178]
111. Willem HK, Patricia LB, Chi VD. Nat. Rev. Cancer. 2011; 11:325. [PubMed: 21508971]
112. Jiang J, Moore J, Edelhauser H, Prausnitz M. Pharm. Res. 2009; 26:395. [PubMed: 18979189]
113. Zhang Y, So MK, Rao J. Nano Lett. 2006; 6:1988. [PubMed: 16968013]
114. Edward B, Trevor M, Emmanuelle d, Alain P, Brian S, Yves B, et al. Nat. Med. 2003; 9:796. [PubMed: 12754503]
115. Kuhn SJ, Finch SK, Hallahan DE, Giorgio TD. Nano Lett. 2006; 6:306. [PubMed: 16464055]
116. Eikenes L, Tari M, Tufto I, Bruland ØS, Davies CdL. Br. J. Cancer. 2005; 93:81. [PubMed: 15942637]
117. Goodman TT, Chen J, Matveev K, Pun SH. Biotechnol. Bioeng. 2008; 101:388. [PubMed: 18500767]
118. Kessenbrock K, Plaks V, Werb Z. Cell. 2010; 141:52. [PubMed: 20371345]
119. Mansour AM, Drevs J, Esser N, Hamada FM, Badary OA, Unger C, et al. Cancer Res. 2003; 63:4062. [PubMed: 12874007]
120. Chau Y, Padera RF, Dang NM, Langer R. Int. J. Cancer. 2006; 118:1519. [PubMed: 16187287]

121. Zhu L, Wang T, Perche F, Taigind A, Torchilin VP. Proc. Natl. Acad. Sci. U.S.A. 2013; 110:17047. [PubMed: 24062440]
122. Maeda H, Noguchi Y, Sato K, Akaike T. Cancer Sci. 1994; 85:331.
123. Nagamitsu A, Greish K, Maeda H. Jpn. J. Clin. Oncol. 2009; 39:756. [PubMed: 19596662]
124. Seki T, Fang J, Maeda H. Cancer Sci. 2009; 100:2426. [PubMed: 19793083]
125. Heldin CH, Rubin K, Pietras K, Östman A. Nat. Rev. Cancer. 2004; 4:806. [PubMed: 15510161]
126. Seynhaeve ALB, Hoving S, Schipper D, Vermeulen CE, De Wiel-Ambagtsheer GA, Van Tiel ST, et al. Cancer Res. 2007; 67:9455. [PubMed: 17909055]
127. Li C, Ke S, Wu QP, Tansey W, Hunter N, Buchmiller LM, et al. Clin. Cancer Res. 2000; 6:2829. [PubMed: 10914731]
128. Davies, CdL; Lundstrøm, LM.; Frengen, J.; Eikenes, L.; Bruland, ØS.; Kaalhus, O., et al. Cancer Res. 2004; 64:547. [PubMed: 14744768]
129. Putnam D, Zelikin AN, Izumrudov VA, Langer R. Biomaterials. 2003; 24:4425. [PubMed: 12922153]
130. Lee ES, Na K, Bae YH. J. Controlled Release. 2003; 91:103.
131. Lee ES, Na K, Bae YH. J. Controlled Release. 2005; 103:405.
132. Sethuraman VA, Bae YH. J. Controlled Release. 2007; 118:216.
133. Lee ES, Kim D, Youn YS, Oh KT, Bae YH. Angew. Chem. Int. Ed. 2008; 47:2418.
134. Sabharanjak S, Mayor S. Adv. Drug Delivery Rev. 2004; 56:1099.
135. Sawant RM, Hurley JP, Salmaso S, Kale A, Tolcheva E, Levchenko TS, et al. Bioconjugate Chem. 2006; 17:943.
136. Zaman NT, Yang Y-Y, Ying JY. Nano Today. 2010; 5:9.
137. Farokhzad OC, Cheng J, Teply BA, Sherifi I, Jon S, Kantoff PW, et al. Proc. Natl. Acad. Sci. U.S.A. 2006; 103:6315. [PubMed: 16606824]
138. Sonawane ND, Szoka FC, Verkman AS. J. Biol. Chem. 2003; 278:44826. [PubMed: 12944394]
139. Straubinger RM, Düzgünes N, Papahadjopoulos D. FEBS Lett. 1985; 179:148. [PubMed: 2578112]
140. Fischer R, Köhler K, Fotin-Mleczek M, Brock R. J. Biol. Chem. 2004; 279:12625. [PubMed: 14707144]
141. Li W, Nicol F, Szoka FC Jr. Adv. Drug Delivery Rev. 2004; 56:967.
142. Murthy N, Campbell J, Fausto N, Hoffman AS, Stayton PS. Bioconjugate Chem. 2003; 14:412.
143. Park JS, Han TH, Lee KY, Han SS, Hwang JJ, Moon DH, et al. J. Controlled Release. 2006; 115:37.
144. Rikke VB, Maria AM, Jonas RH, Moghimi SM, Thomas LA. Mol. Ther. 2012; 21:149. [PubMed: 23032976]
145. Berg K, Kristian Selbo P, Prasmickaite L, Tjelle TE, Sandvig K, Moan J, et al. Cancer Res. 1999; 59:1180. [PubMed: 10096543]
146. Yamada Y, Harashima H. Adv. Drug Delivery Rev. 2008; 60:1439.
147. Callahan J, Kopeček J. Biomacromolecules. 2006; 7:2347. [PubMed: 16903681]
148. Marrache S, Dhar S. Proc. Natl. Acad. Sci. U.S.A. 2012; 109:16288. [PubMed: 22991470]
149. D'Souza GG, Cheng S-M, Boddapati SV, Horobin RW, Weissig V. J. Drug Targeting. 2008; 16:578.
150. Lukacs GL, Haggie P, Seksek O, Lechardeur D, Freedman N, Verkman AS. J. Biol. Chem. 2000; 275:1625. [PubMed: 10636854]
151. Chee-Kai C, David AJ. Immunol. Cell Biol. 2002; 80:119. [PubMed: 11940112]
152. Chen HH, Ho Y-P, Jiang X, Mao H-Q, Wang T-H, Leong KW. Nano Today. 2009; 4:125. [PubMed: 20161048]
153. Miller AM, Dean DA. Gene Ther. 2008; 15:1107. [PubMed: 18496575]
154. Hoang B, Ekdawi SN, Reilly RM, Allen C. Mol. Pharm. 2013; 10:4229. [PubMed: 24066900]
155. Lentacker I, Vandenbroucke RE, Lucas B, Demeester J, De Smedt SC, Sanders NN. J. Controlled Release. 2008; 132:279.

156. Vandenbroucke RE, Lucas B, Demeester J, De Smedt SC, Sanders NN. Nucleic Acids Res. 2007; 35:e86. [PubMed: 17584788]
157. Jong Ah K, Christoffer Å, Anna S, Kenneth AD. Nat. Nanotechnol. 2011; 7:62. [PubMed: 22056728]
158. Carlee EA, Eric CC, Genevieve KP, David P, Paul ND, Page AB, et al. Nat. Mater. 2011; 10:389. [PubMed: 21499315]
159. Thapa RBKCB, Xu P. Mol. Pharm. 2012; 9:2719. [PubMed: 22876763]
160. Panyam J, Zhou W-Z, Prabha S, Sahoo SK, Labhasetwar V. FASEB J. 2002; 16:1217. [PubMed: 12153989]
161. Muro S, Cui X, Gajewski C, Murciano J-C, Muzykantov VR, Koval M. Am. J. Physiol. 2003; 285:C1339.
162. José MM, Enas AM, Jagadis S, Adah A. J. Drug Deliv. 2012; 2012
163. Obermajer N, Kocbek P, Repnik U, Kužnik A, Cegnar M, Kristl J, et al. FEBS J. 2007; 274:4416. [PubMed: 17662106]
164. Cajot S, Van Butsele K, Paillard A, Passirani C, Garcion E, Benoit JP, et al. Acta Biomaterialia. 2012; 8:4215. [PubMed: 22963850]
165. Greco F, Vicent MJ, Gee S, Jones AT, Gee J, Nicholson RI, et al. J. Controlled Release. 2007; 117:28.
166. Duncan R, Sat-Klopsch Y-N, Burger A, Bibby M, Fiebig H, Sausville E. Cancer Chemother. Pharmacol. 2013; 72:417. [PubMed: 23797686]
167. Park, JB.; Lakes, RS. Biomaterials: An Introduction. 3rd ed.. New York: Springer; 2007.
168. Bouwstra JA, Honeywell-Nguyen PL. Adv. Drug Delivery Rev. 2002; 54(Supplement):S41.
169. Christophers E. J. Invest. Dermatol. 1971; 56:165. [PubMed: 4104137]
170. Naik A, Kalia YN, Guy RH. Pharm. Sci. Technol. Today. 2000; 3:318. [PubMed: 10996573]
171. Tezel A, Paliwal S, Shen Z, Mitragotri S. Vaccine. 2005; 23:3800. [PubMed: 15893617]
172. Tezel A, Dokka S, Kelly S, Hardee GE, Mitragotri S. Pharm. Res. 2004; 21:2219. [PubMed: 15648253]
173. Sanders NN, De Smedt SC, Van Rompaey E, Simoens P, De Baets F, Demeester J. Am. J. Respir. Crit. Care Med. 2000; 162:1905. [PubMed: 11069833]
174. Shah PP, Desai PR, Singh M. J. Controlled Release. 2012; 158:336.
175. Desai PR, Marepally S, Patel AR, Voshavar C, Chaudhuri A, Singh M. J. Controlled Release. 2013; 170:51.
176. Prausnitz MR, Langer R. Nature biotechnology. 2008; 26:1261.
177. Prausnitz MR, Mitragotri S, Langer R. Nature reviews. Drug discovery. 2004; 3:115.
178. Honeywell-Nguyen PL, Bouwstra JA. Drug Discov. Today Technol. 2005; 2:67. [PubMed: 24981757]
179. De Leeuw J, De Vijlder HC, Bjerring P, Neumann HAM. J. Eur. Acad. Dermatol. Venereol. 2009; 23:505. [PubMed: 19175703]
180. Elsayed MMA, Abdallah OY, Naggar VF, Khalafallah NM. Int. J. Pharm. 2007; 332:1. [PubMed: 17222523]
181. Shen L-N, Zhang Y-T, Wang Q, Xu L, Feng N-P. Int. J. Pharm.
182. Rakesh R, Anoop KR. J. Pharm. Bioallied. Sci. 4
183. Zhang Z, Wo Y, Zhang Y, Wang D, He R, Chen H, et al. Nanomed. Nanotechnol. Biol. Med. 2012; 8:1026.
184. Ghanbarzadeh S, Arami S. Biomed. Res. Int. 2013; 2013:7.
185. Raza K, Singh B, Lohan S, Sharma G, Negi P, Yachha Y, et al. Int. J. Pharm. 2013; 456:65. [PubMed: 23973754]
186. Sinico C, Fadda AM. Expert Opin. Drug Deliv. 2009; 6:813. [PubMed: 19569979]
187. Oh Y-K, Kim MY, Shin J-Y, Kim TW, Yun M-O, Yang SJ, et al. J. Pharm. Pharmacol. 2006; 58:161. [PubMed: 16451743]
188. Abdelwahed W, Degobert G, Stainmesse S, Fessi H. Adv. Drug Delivery Rev. 2006; 58:1688.

189. Khurana S, Bedi PMS, Jain NK. Chem. Phys. Lipids. 2013; 175–176:65.
190. Shiva G, Somaye M, Reza Jaafari M. Acta Pharmaceutica. 2012; 62:547. [PubMed: 23333889]
191. Santander-Ortega MJ, Stauner T, Loretz B, Ortega-Vinuesa JL, Bastos-González D, Wenz G, et al. J. Controlled Release. 2010; 141:85.
192. Wang X, Zheng C, Wu Z, Teng D, Zhang X, Wang Z, et al. J. Biomed. Mater. Res. B Appl. Biomater. 2009; 88B:150. [PubMed: 18618466]
193. Rancan F, Papakostas D, Hadam S, Hackbarth S, Delair T, Primard C, et al. Pharm. Res. 2009; 26:2027. [PubMed: 19533305]
194. Janesirisakule S, Sinthusake T, Wanichwecharungruang S. J. Pharm. Sci. 2013; 102:2770. [PubMed: 23775704]
195. Mittal A, Raber AS, Schaefer UF, Weissmann S, Ebensen T, Schulze K, et al. Vaccine. 2013; 31:3442. [PubMed: 23290836]
196. Bal SM, Slütter B, van Riet E, Kruithof AC, Ding Z, Kersten GFA, et al. J. Controlled Release. 2010; 142:374.
197. Brooks H, Lebleu B, Vivès E. Adv. Drug Delivery Rev. 2005; 57:559.
198. Zorko M, Langel Ü. Adv. Drug Delivery Rev. 2005; 57:529.
199. Hsu T, Mitragotri S. Proc. Natl. Acad. Sci. U.S.A. 2011; 108:15816. [PubMed: 21903933]
200. Chen M, Gupta V, Anselmo AC, Muraski JA, Mitragotri S. J. Controlled Release. 2014; 173:67.
201. Washington, N.; Washington, C.; Wilson, C. Physiological Pharmaceutics: Barriers to Drug Absorption ed. Taylor & Francis; 2000.
202. Cohen M, Zhang XQ, Senaati HP, Chen HW, Varki NM, Schooley RT, et al. Virol. J. 2013; 10:321. [PubMed: 24261589]
203. Lai SK, Wang Y-Y, Hanes J. Adv. Drug Delivery Rev. 2009; 61:158.
204. Round AN, Rigby NM, Garcia de la Torre A, Macierzanka A, Mills ENC, Mackie AR. Biomacromolecules. 2012; 13:3253. [PubMed: 22978827]
205. Ensign LM, Hoen TE, Maisel K, Cone RA, Hanes JS. Biomaterials. 2013; 34:6922. [PubMed: 23769419]
206. Lai SK, O'Hanlon DE, Harrold S, Man ST, Wang Y-Y, Cone R, et al. Proc. Natl. Acad. Sci. U.S.A. 2007; 104:1482. [PubMed: 17244708]
207. Tang BC, Dawson M, Lai SK, Wang Y-Y, Suk JS, Yang M, et al. Proc. Natl. Acad. Sci. U.S.A. 2009; 106:19268. [PubMed: 19901335]
208. Wang Y-Y, Lai SK, Ensign LM, Zhong W, Cone R, Hanes J. Biomacromolecules. 2013; 14:4429. [PubMed: 24266646]
209. Yamanaka YJ, Leong KW. J. Biomech. 2008; 19:1549.
210. Damgé C, Michel C, Aprahamian M, Couvreur P, Devissaguet JP. J. Controlled Release. 1990; 13:233.
211. Noh Y-W, Hong JH, Shim S-M, Park HS, Bae HH, Ryu EK, et al. Angew. Chem. Int. Ed. 2013; 52:7684.
212. He C, Yin L, Tang C, Yin C. Biomaterials. 2012; 33:8569. [PubMed: 22906606]
213. Teubl BJ, Meindl C, Eitzlmayr A, Zimmer A, Fröhlich E, Roblegg E. Small. 2013; 9:457. [PubMed: 23112142]
214. das Neves J, Rocha CMR, Gonçalves MP, Carrier RL, Amiji M, Bahia MF, et al. Mol. Pharm. 2012; 9:3347. [PubMed: 23003680]
215. Wang Y-Y, Lai SK, So C, Schneider C, Cone R, Hanes J. PLoS ONE. 2011; 6:e21547. [PubMed: 21738703]
216. Hermanson, GT. Bioconjugate techniques ed. Amsterdam [Netherlands]; Boston [Mass.]: Academic Press; 2008.
217. Henning A, Schneider M, Nafee N, Muijs L, Rytting E, Wang X, et al. J. Aerosol. Med. Pulm. Drug Deliv. 2010; 23:233. [PubMed: 20500091]
218. Cu Y, Saltzman WM. Mol. Pharm. 2008; 6:173. [PubMed: 19053536]
219. Wang Y-Y, Lai SK, Suk JS, Pace A, Cone R, Hanes J. Angew. Chem. Int. Ed. 2008; 47:9726.
220. Goldberg DS, Vijayalakshmi N, Swaan PW, Ghandehari H. J. Controlled Release. 2011; 150:318.

221. Ensign LM, Cone R, Hanes J. Adv. Drug Delivery Rev. 2012; 64:557.
222. Albanese CT, Cardona M, Smith SD, Watkins S, Kurkchubasche AG, Ulman I, et al. Surgery. 1994; 116:76. [PubMed: 8023272]
223. Gaucher G, Satturwar P, Jones M-C, Furtos A, Leroux J-C. Eur. J. Pharm. Biopharm. 2010; 76:147. [PubMed: 20600891]
224. Nguyen H-N, Wey S-P, Juang J-H, Sonaje K, Ho Y-C, Chuang E-Y, et al. Biomaterials. 2011; 32:2673. [PubMed: 21256586]
225. Li X, Guo S, Zhu C, Zhu Q, Gan Y, Rantanen J, et al. Biomaterials. 2013; 34:9678. [PubMed: 24016855]
226. Sutton D, Nasongkla N, Blanco E, Gao J. Pharm. Res. 2007; 24:1029. [PubMed: 17385025]
227. Khutoryanskiy VV. Macromol. Biosci. 2011; 11:748. [PubMed: 21188688]
228. Kitchens KM, Kolhatkar RB, Swaan PW, Ghandehari H. Mol. Pharm. 2008; 5:364. [PubMed: 18173246]
229. Goldberg D, Ghandehari H, Swaan P. Pharm. Res. 2010; 27:1547. [PubMed: 20411406]
230. Jevprasesphant R, Penny J, Attwood D, McKeown N, D'Emanuele A. Pharm. Res. 2003; 20:1543. [PubMed: 14620505]
231. Kraehenbuhl JP, Neutra MR. Annu. Rev. Cell Dev. Biol. 2000; 16:301. [PubMed: 11031239]
232. Groo AC, Saulnier P, Gimel JC, Gravier J, Ailhas C, Benoit JP, et al. Int. J. Nanomedicine. 2013; 8:4291. [PubMed: 24235827]
233. Liu D, Bimbo LM, Mäkilä E, Villanova F, Kaasalainen M, Herranz-Blanco B, et al. J. Controlled Release. 2013; 170:268.
234. Yuan H, Chen C-Y, Chai G-h, Du Y-Z, Hu F-Q. Mol. Pharm. 2013; 10:1865. [PubMed: 23495754]
235. Yin Y, Chen D, Qiao M, Wei X, Hu H. J. Controlled Release. 2007; 123:27.
236. Khan MZI, Prebeg Ž, Kurjaković N. J. Controlled Release. 1999; 58:215.
237. Jin Y, Song Y, Zhu X, Zhou D, Chen C, Zhang Z, et al. Biomaterials. 2012; 33:1573. [PubMed: 22093292]
238. Pridgen EM, Alexis F, Kuo TT, Levy-Nissenbaum E, Karnik R, Blumberg RS, et al. Science translational medicine. 2013; 5:213ra167.
239. Knowles MR, Boucher RC. J. Clin. Invest. 2002; 109:571. [PubMed: 11877463]
240. Jeon JO, Kim S, Choi E, Shin K, Cha K, So I-S, et al. ACS Nano. 2013; 7:7462. [PubMed: 23927443]
241. Lawson KA, Anderson K, Snyder RM, Simmons-Menchaca M, Atkinson J, Sun LZ, et al. Cancer Chemother. Pharmacol. 2004; 54:421. [PubMed: 15197487]
242. Kawashima Y, Yamamoto H, Takeuchi H, Fujioka S, Hino T. J. Controlled Release. 1999; 62:279.
243. Zhang Q, Shen Z, Nagai T. Int. J. Pharm. 2001; 218:75. [PubMed: 11337151]
244. Liu J, Gong T, Fu H, Wang C, Wang X, Chen Q, et al. Int. J. Pharm. 2008; 356:333. [PubMed: 18281169]
245. Pandey R, Khuller GK. Tuberculosis. 2005; 85:227. [PubMed: 15922668]
246. Bali, V.; Singh, S.; Kumar, A. Patenting Nanomedicines. Souto, EB., editor. Heidelberg: Springer Berlin; 2012. p. 251-275.
247. Illum L. J. Controlled Release. 2012; 161:254.
248. das Neves J, Amiji M, Sarmento B. Wiley Interdiscip. Rev. Nanomed. Nanobiotechnol. 2011; 3:389. [PubMed: 21506290]
249. Kim AJ, Boylan NJ, Suk JS, Hwangbo M, Yu T, Schuster BS, et al. Angew. Chem. Int. Ed. 2013; 52:3985.
250. Chiu JJ, Chien S. Physiol. Rev. 2011; 91:327. [PubMed: 21248169]
251. Paguirigan A, Beebe DJ. Lab Chip. 2006; 6:407. [PubMed: 16511624]
252. Baker BM, Trappmann B, Stapleton SC, Toro E, Chen CS. Lab Chip. 2013; 13:3246. [PubMed: 23787488]

253. Ling Y, Rubin J, Deng Y, Huang C, Demirci U, Karp JM, et al. Lab Chip. 2007; 7:756. [PubMed: 17538718]

254. Du Y, Ghodousi M, Qi H, Haas N, Xiao W, Khademhosseini A. Biotechnol. Bioeng. 2011; 108:1693. [PubMed: 21337336]

255. Zervantonakis IK, Hughes-Alford SK, Charest JL, Condeelis JS, Gertler FB, Kamm RD. Proc. Natl. Acad. Sci. U.S.A. 2012

256. Prabhakarpandian B, Shen M-C, Nichols JB, Mills IR, Sidoryk-Wegrzynowicz M, Aschner M, et al. Lab Chip. 2013; 13:1093. [PubMed: 23344641]

257. Karande P, Mitragotri S. Annu. Rev. Chem. Biomol. Eng. 2010; 1:175. [PubMed: 22432578]

Highlights

- Transport barriers for delivery of nanoparticles are discussed
- Permeation across the endothelium, diffusion in the interstitium and entry into cells is discussed
- Permeation of nanoparticles across the skin and mucosal membranes is discussed

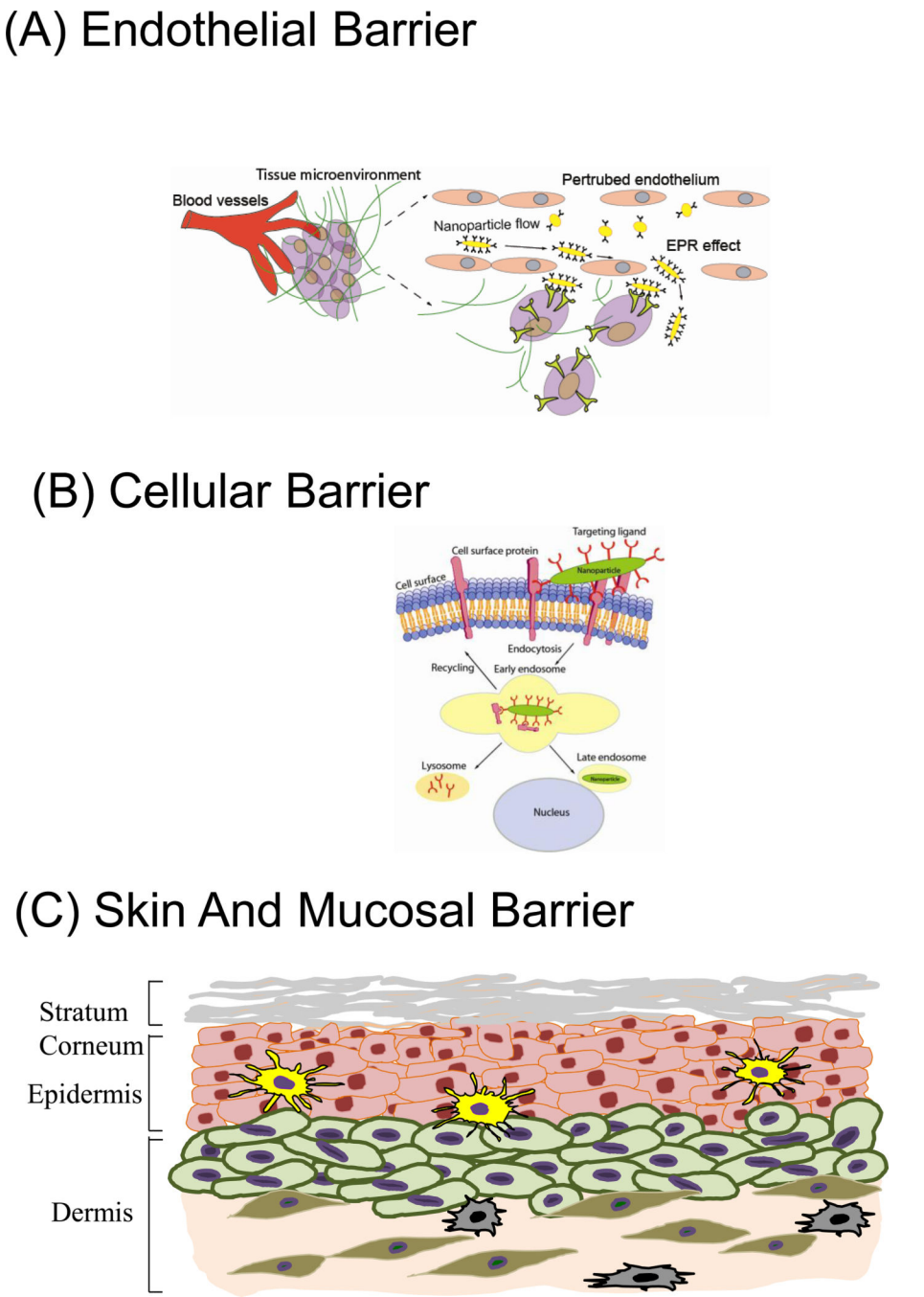

Figure 1.

The major barriers at the **(A)** endothelium, **(B)** cellular, **(C)** skin level that NPs face during their transport to target cells. **(A)** NPs after intravenous injection circulate throughout the body and accumulate in the tumor passively through enhanced permeation and retention (EPR) effect. **(B)** Once the NPs are extravasated from the blood to the tumor site, it must bind to the cell membrane following an efficient entry inside the cell (endocytosis). NPs are then localized in late endosomes and nucleus, degraded in lysosomes or recycled back to the

plasma membrane. **(C)** Skin poses the outer layer barrier to the body consisting of three layers: the *stratum corneum*epidermis and dermis. Figure **(C)** is taken from Ref. [257].

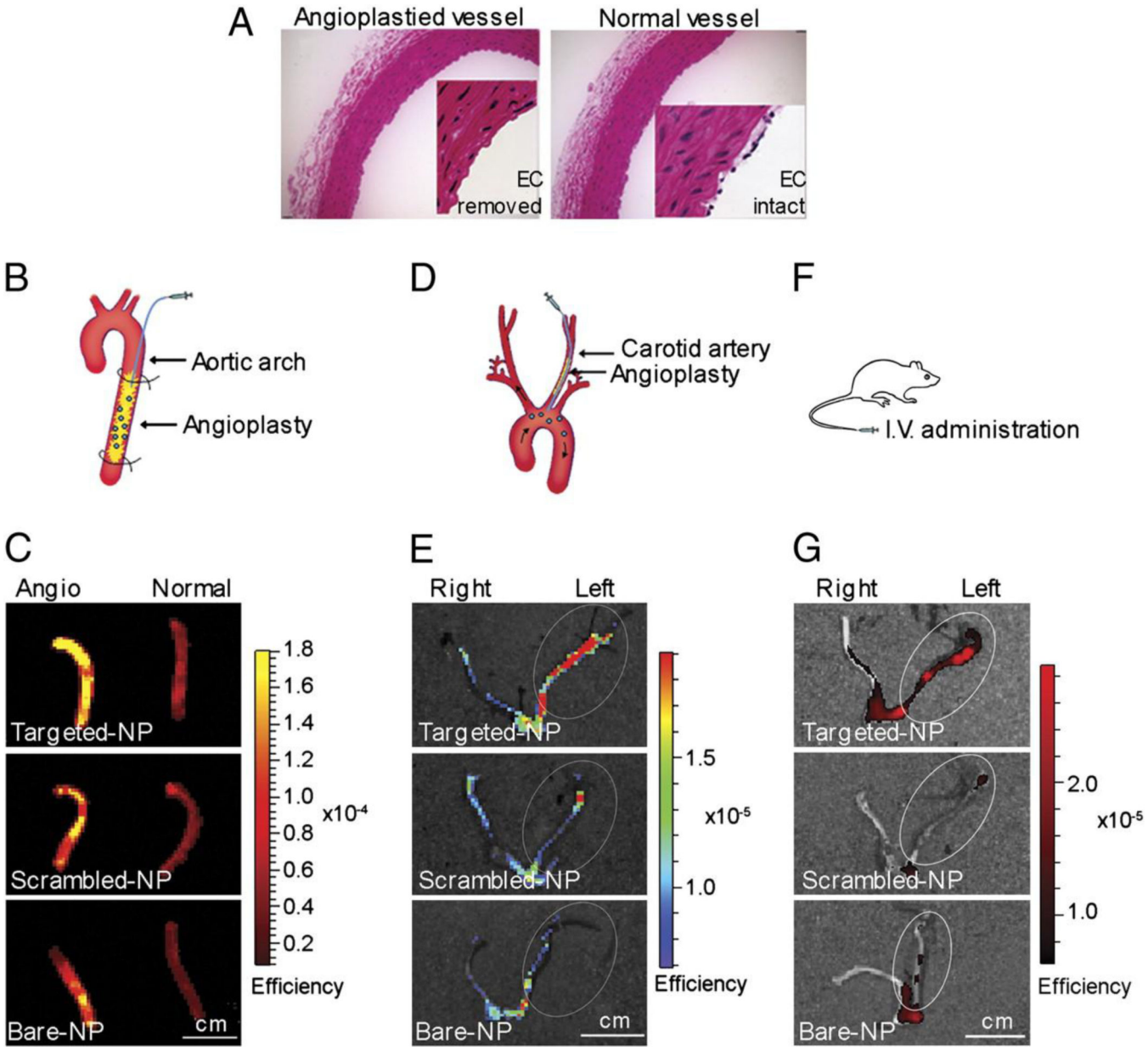

Figure 2.

PTX delivery using polymeric NPs showed greater *in vivo* vascular retention than untargeted controls [42]. (A) H& E staining of an uninjured aorta and injured aorta with the endothelial layer removed. Schematic images of NPs delivered to (B) an abdominal aorta and (D) a left carotid injury (F) of a mouse model. (C) Fluorescence microscopic images of Alexa 647 dye conjugated PLGA targeting intact endothelial layers and injured aortas. (E) Left carotid arteries showed four fold more NPs than healthy right carotids. (G) NP retention was higher in left carotids than untargeted NPs (Figures from Ref. [42])

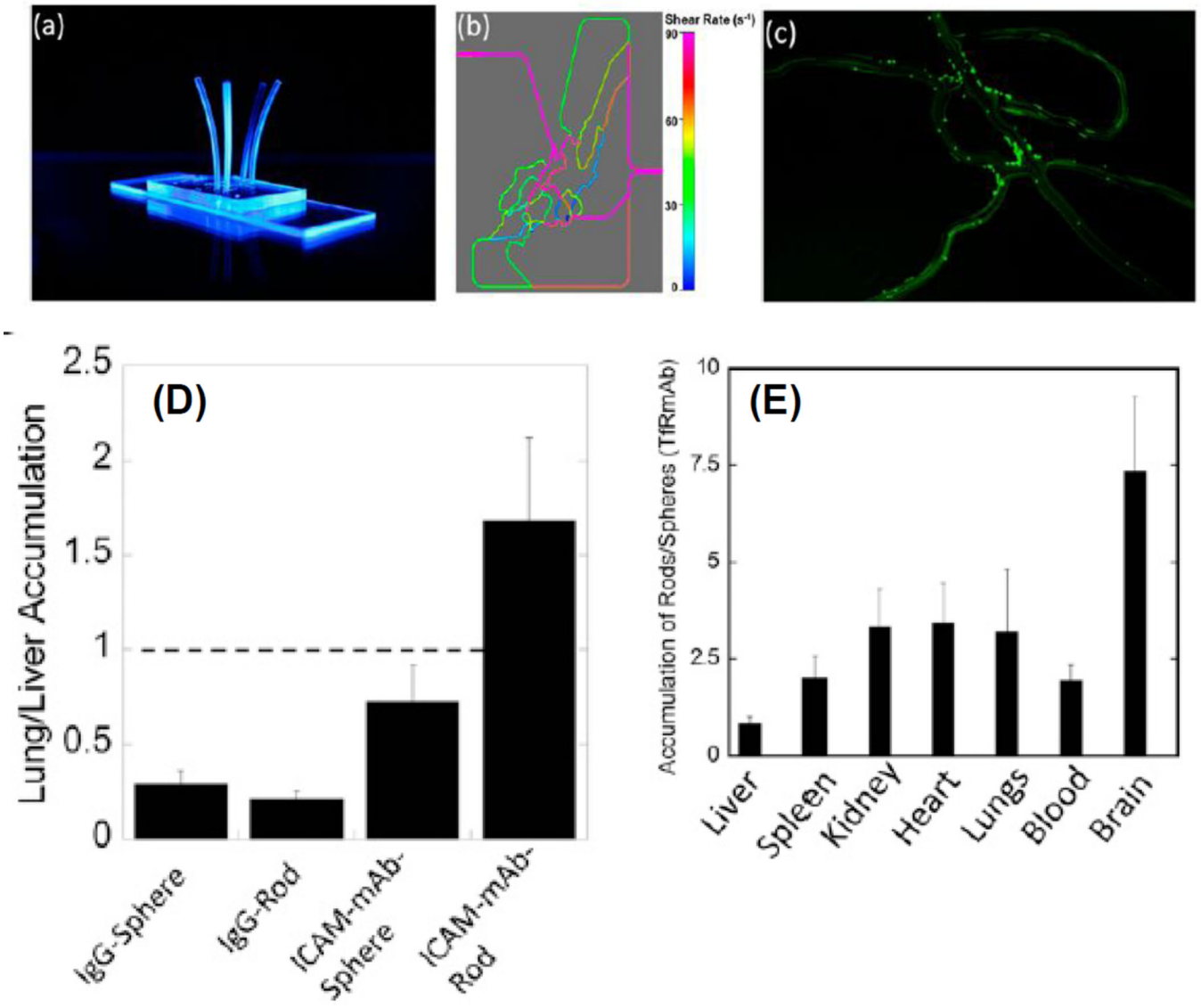

Figure 3.

NP shape induced targeting of vascular endothelium as observed in synthetic microvascular networks (SMN) *in vitro* and lung and brain targeting *in vivo* [77]. **(A)** and **(B)** The SMN device incorporates the vascular physiology and shear rates on endothelial cell monolayer. **(C)** NPs coated with anti-OVA antibody adhere to the vascular channels of SMN when the channels are coated with OVA mimicking the specific interactions between targeted NPs and the vascular channels. **(D)** *In vivo* biodistribution of ICAM antibody coated NPs show preferential accumulation of lungs compared to liver. ICAM-coated nanorods show ~2-fold higher lung/liver ratio than ICAM-coated spheres. **(E)** Tf-coated nanorods accumulate in the brain ~7.5-fold more than Tf-coated spheres. (Figured from Ref. [77]).

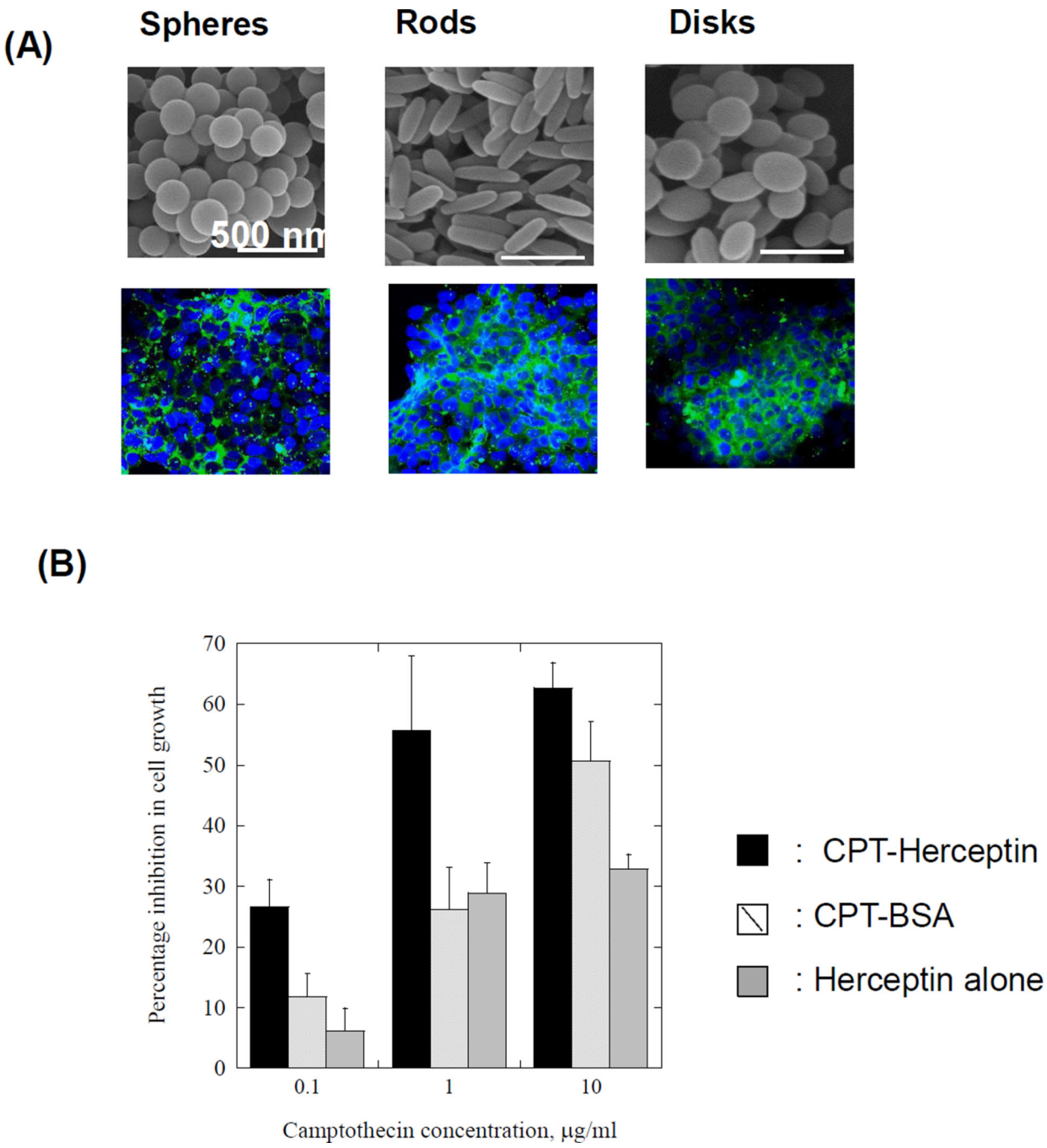

Figure 4.

NP shape affects their cellular uptake and therapeutic activity of the delivered drugs. **(A)** Top row: Scanning electron microscopy of spherical, rod and disk shaped particles prepared using film stretching method [69, 76]. Bottom row: Confocal microscopic images of intracellular uptake of spherical, rod and disk shaped particles after herceptin antibody coating [76]. Herceptin-coated rod-shaped NPs were taken up the most by BT-474 breast cancer cells. **(B)** Cancer cell growth inhibition data using Herceptin coated rods and spheres. Herceptin-coated rods (10 μg/ml) inhibited BT-474 breast cancer cell growth up to 50%

using only 1 μg/ml herceptin presented on the particles. **(C)** Herceptin-coated CPT drug nanorods inhibited BT-474 cell growth synergistically using only 1 μg/ml CPT and 0.16 μg/ml hercpetin. Figures from Ref. [76]).

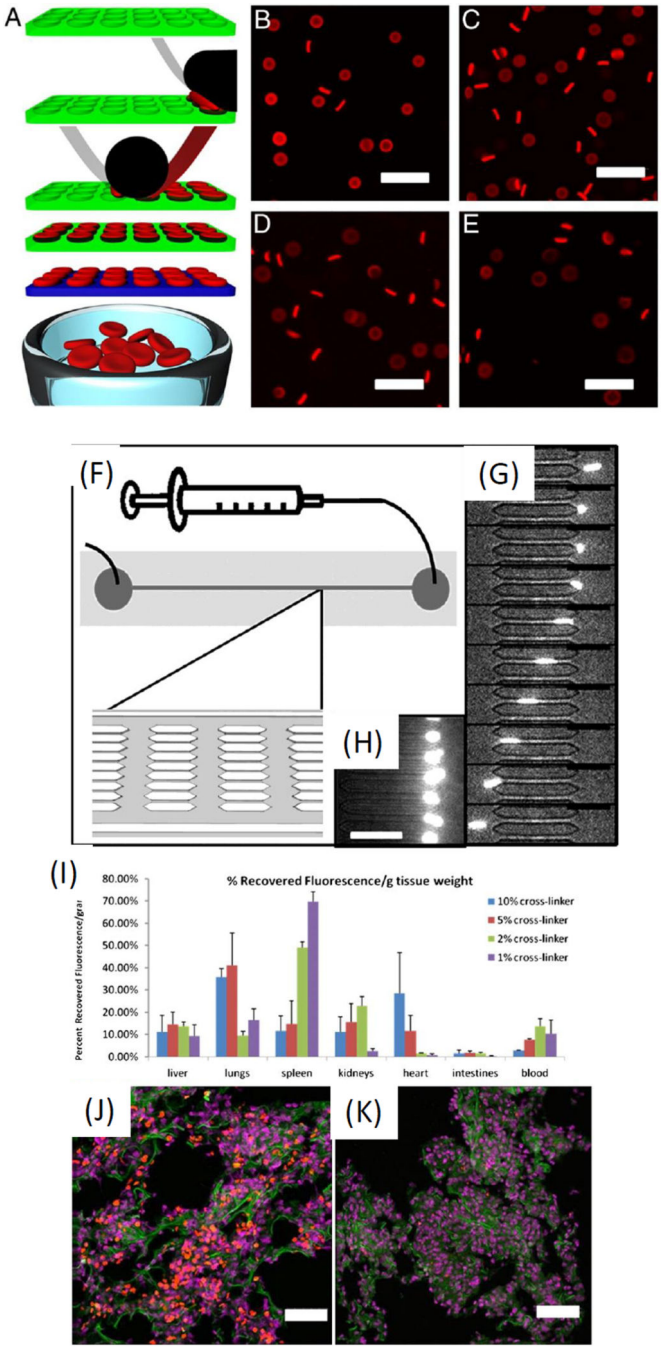

Figure 5.

(A) RBC particle prepared by PRINT technology [97]. **(B–E)** Fluorescent images of RBCs with varying percent of cross-linkers. (F–H) RBC deformation in flow conditions. (I) Biodistribution of RBCs in mouse. **(J–H)** RBC particles (red) in lung tissues (purple: nuclei and green: F-actin). Scale bar=50μm (Figures from Ref. [97]).

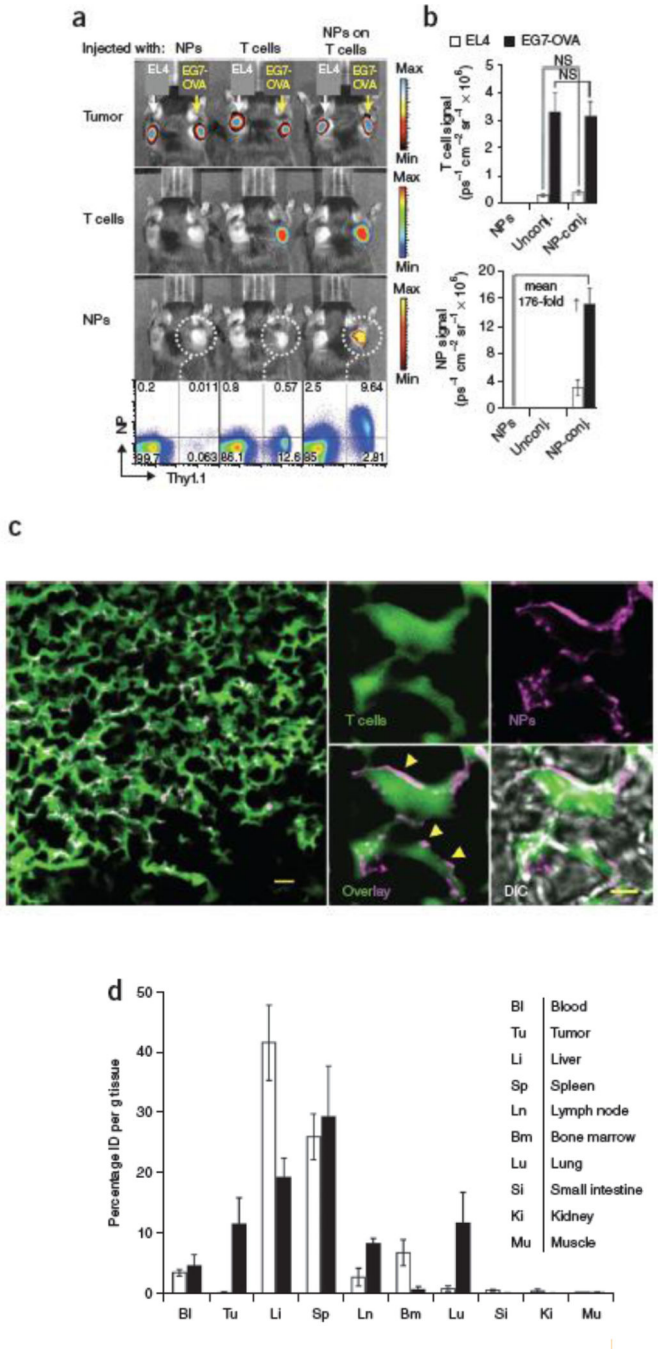

Figure 6.

Tumor homing of particle conjugated lymphocytes [99]. **(A)** Particle carrying T cells trafficked to EL4-OVA tumors. **(B)** No difference in the tumor homing potential of particle conjugated T cells versus unmodified OT-1 T cells. **(C)** Infiltration of NP decorated T cells into EG7-OVA tumors as determined by confocal microscopy. **(D)** Quantitative analysis particle-decorated and control OT-1 cells in tumors (Figures from Ref. [99]).

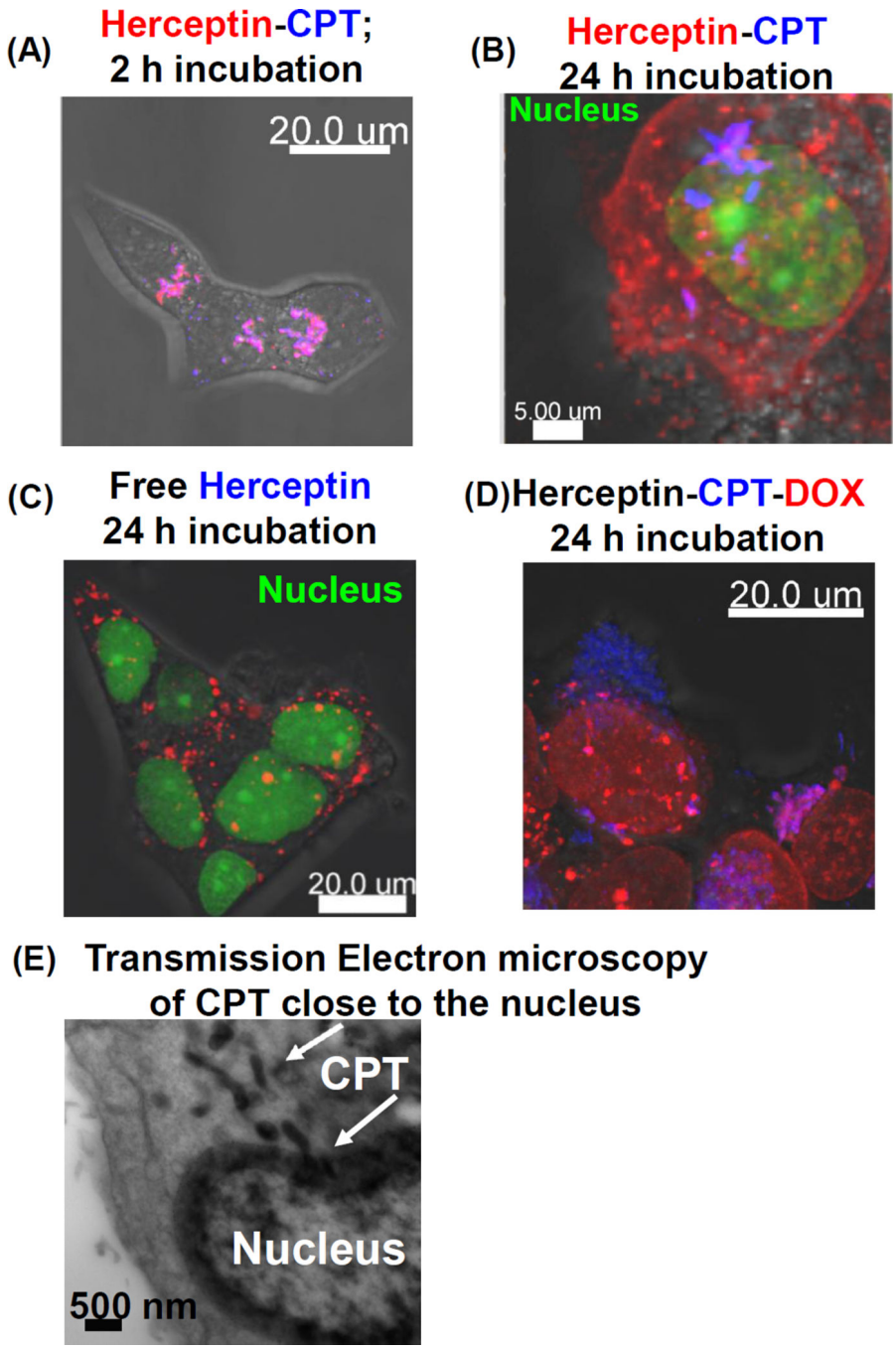

Figure 7.

Confocal and transmission electron microscopic (TEM) images of intracellular distribution and subcellular targeting of Herceptin-coated camptothecin (CPT) drug nanorods in BT-474 breast cancer cells [75]. **(A)** Herceptin (red fluorescence)-coated CPT (blue fluorescence) nanorods enter the cells via receptor-mediated endocytosis. **(B)** Herceptin recycles back to the plasma membrane leaving CPT nanorods inside the cells as observed after 24 h of incubation. CPT nanorods (blue fluorescence) move close to the nucleus as it is seen from the confocal and TEM images. **(C)** Free Herceptin does not show this behavior sitting inside

the cytoplasm even after 24 h. **(D)** DOX (red fluorescence in the Herceptin-CPT-DOX) enters the nucleus when delivered as Herceptin-CPT-DOX nanorods. **(E)** Retention of CPT nanorods close to the nucleus has been confirmed by TEM (Figures from Ref. [75])

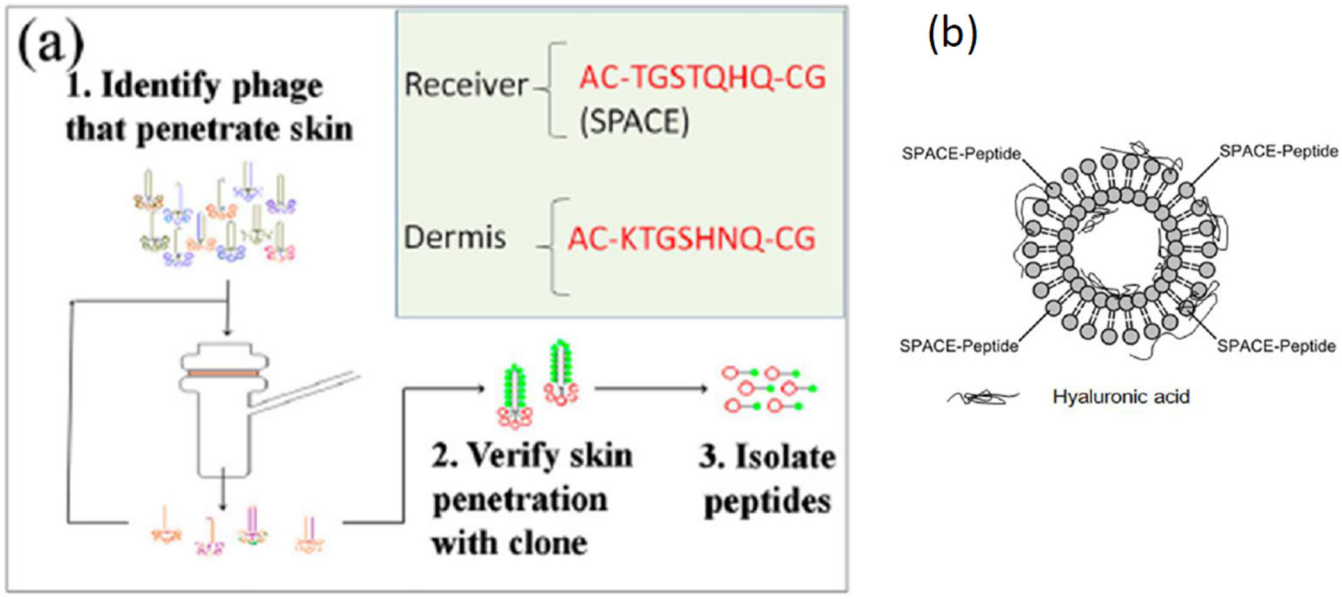

Figure 8.

(A) A cell penetrating peptide, SPACE has been identified using *in vitro* phage display in porcine skin [199]. **(B)** Schematic of an SPACE-decorated ethosome for penetration of siRNA into the skin [200]. (Figures from Refs. [199, 200]).

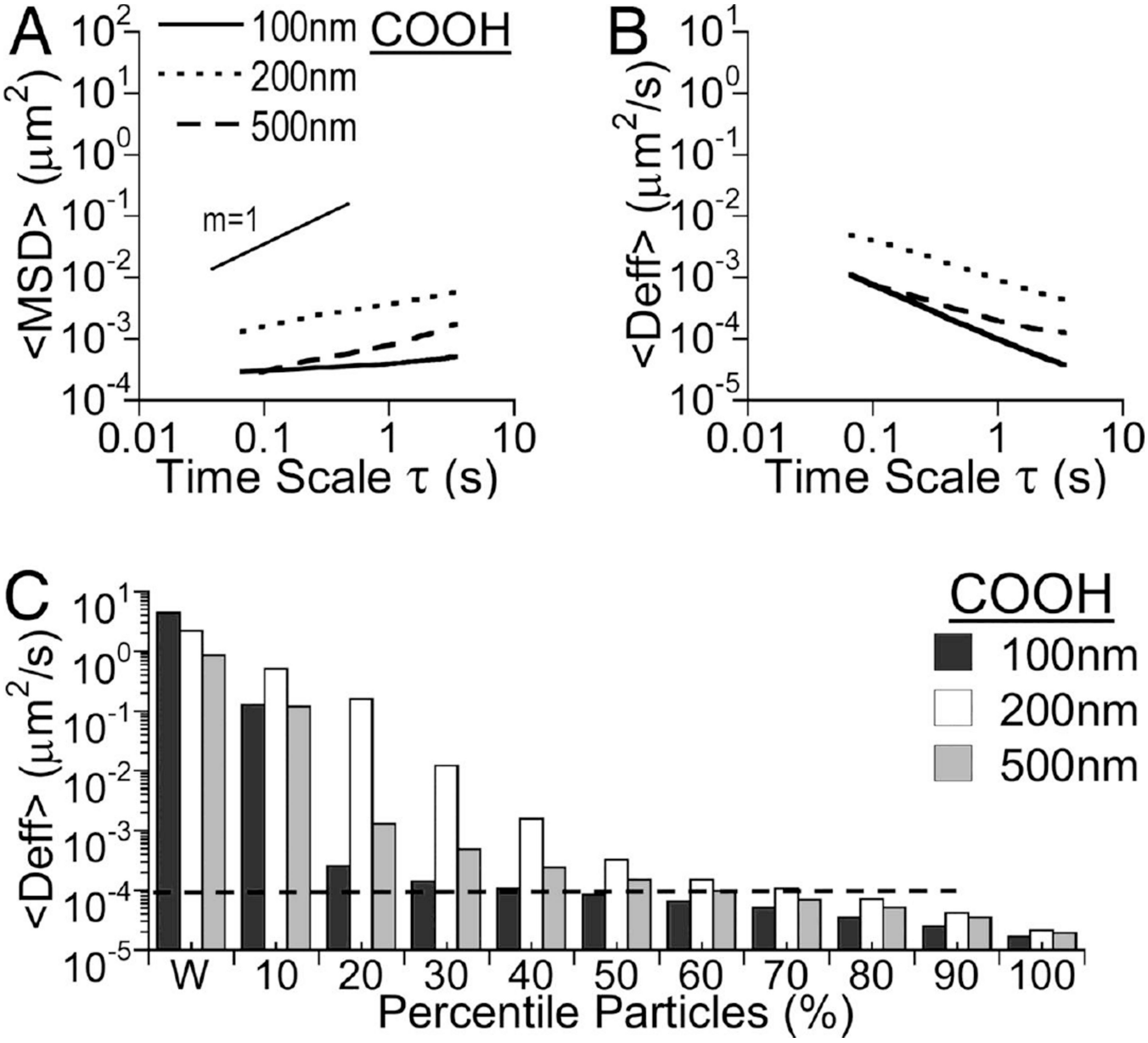

Figure 9.

The effect of particle size on transport rates in cervicovaginal mucus [206]. **(A)** Particle size of 200 and 500 nm showed higher transport rates than 100 nm particles. **(B)** The average effective diffusivity (D_{eff}) of the particles decreased in mucus. **(C)** The mean D_{eff} values were greater for 200 and 500 nm particles than 100 nm particles (Figures from Ref.[206]).

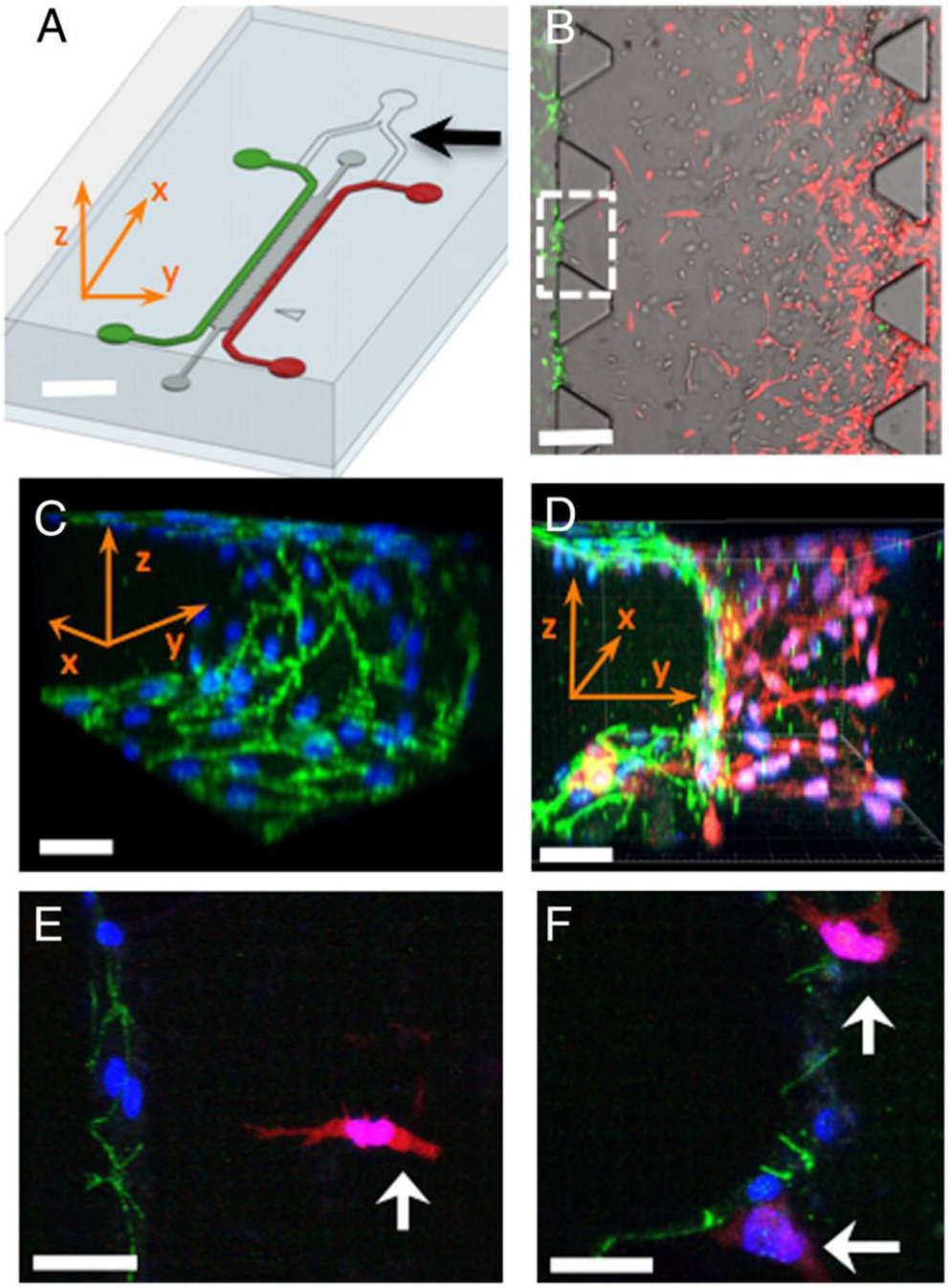

Figure 10.

(A) Microfluidic channel where tumor (red) and endothelial cells (green) were seeded [255]. **(B)** and **(D)** Fibrosarcoma cells (red) invade through the ECM gel (grey) toward the endothelium (green). **(C)** Endothelial cell cell junctions using a vascular endothelial-cadherin antibody. **(E)** and **(F)** Higher magnification images of fibrosarcoma cell migration to tumor cells. (Figures from Ref. [255]).